Determinants of myocardial perfusion - Multimodality imaging in chronic coronary syndrome

Szekely, Anna

2025

Document Version:
Publisher's PDF, also known as Version of record

Determinants of myocardial perfusion

Multimodality imaging in chronic coronary syndrome

ANNA SZÉKELY
DEPARTMENT OF CLINICAL SCIENCES LUND | FACULTY OF MEDICINE | LUND UNIVERSITY

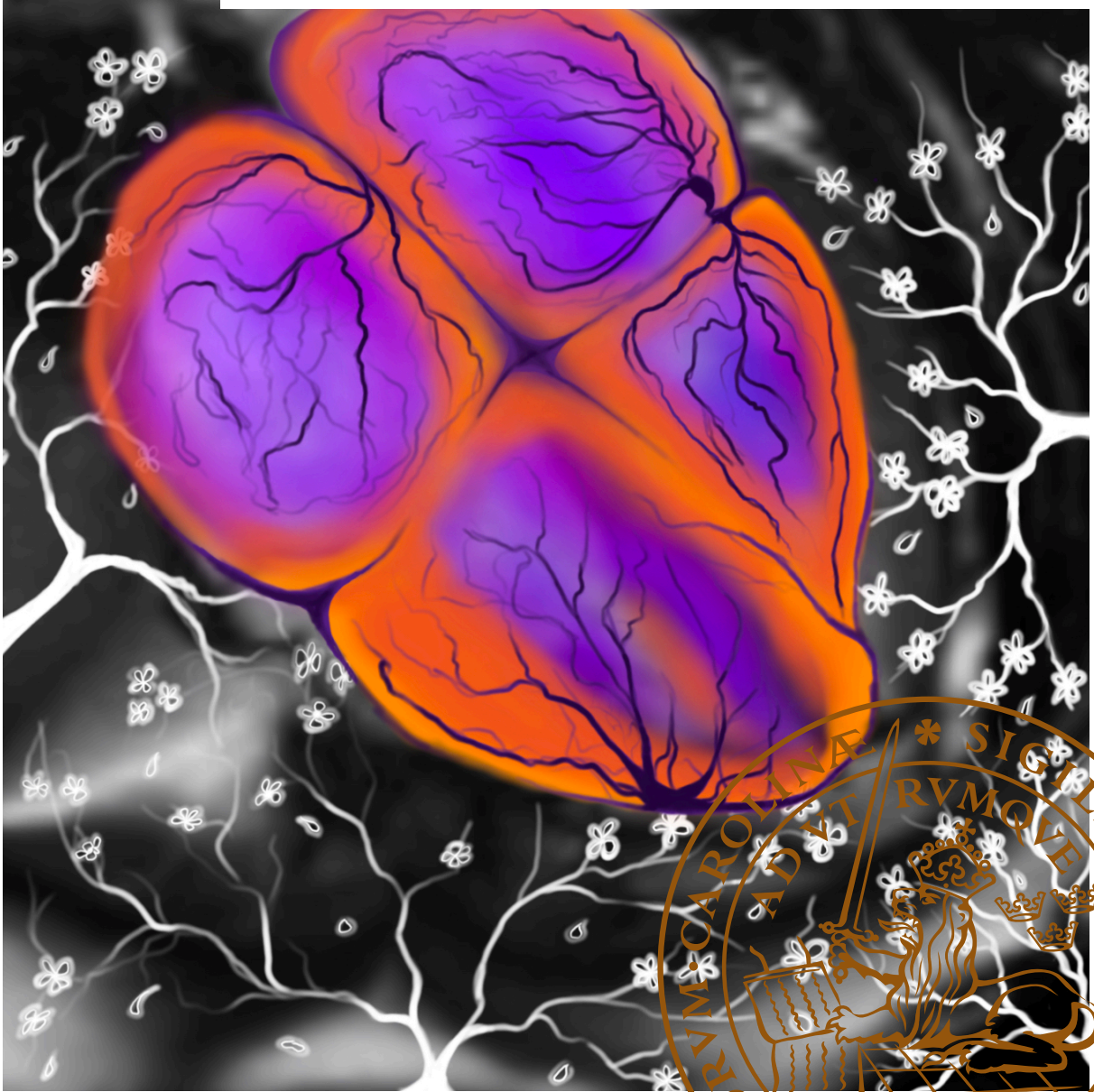

Determinants of myocardial perfusion

Determinants of myocardial perfusion

Multimodality imaging in chronic coronary syndrome

Anna Székely

LUND
UNIVERSITY

DOCTORAL DISSERTATION
Doctoral dissertation for the degree of Doctor of Philosophy (PhD) at the Faculty of Medicine at Lund University to be publicly defended 24th of October 2025 at 9.00 in Segerfalkssalen, Biomedical Centre, Lund University, Sweden.

Thesis advisors: Professor Henrik Engblom and
Associate Professor Katarina Steding-Ehrenborg
Faculty opponent: Professor Juhani Knuuti

Organization
LUND UNIVERSITY

Document name
DOCTORAL DISSERTATION

Date of dissertation
2025-10-24

Sponsoring organization

Author(s)
Anna Székely

Title Determinants of myocardial perfusion - multimodality imaging in chronic coronary syndrome

Abstract
Coronary artery disease is a common disease, affecting millions of people globally. In its stable form, coronary artery disease is called chronic coronary syndrome (CCS). In CCS, the myocardium is not perfused with enough blood when the myocardium's oxygen demand increases, for instance during exercise, due to functional and/or structural alterations of the vessels supplying the myocardium with blood. When the myocardial perfusion does not meet the oxygen demand of the tissue, stress-induced ischemia develops, which can impair cardiac function and lead to symptoms such as angina and dyspnea. According to current clinical guidelines, stress-induced ischemia could be assessed using non-invasive functional imaging prior to invasive coronary angiography (ICA), to avoid unnecessary invasive procedures. Quantitative assessment of myocardial perfusion is possible with quantitative first-pass perfusion (qFPP) cardiac magnetic resonance (CMR) and dynamic cardiac positron emission tomography (PET). Several studies have shown sex differences in the development of CCS, and women are known to have higher myocardial perfusion than men. One potential explanation of this might be the cardioprotective effect of estrogen. The aim of this thesis was to investigate the determinants of myocardial perfusion using different imaging modalities to improve the diagnostics of patients with CCS.

Paper I showed that sex, age, diabetes, hypertension and smoking affect myocardial perfusion independently of the presence of coronary artery stenosis in patients with suspected CCS. Paper II revealed that different reconstruction and post-processing parameters of cardiac PET images affect the absolute perfusion values. The results of Paper III showed that visual assessment of ICA has limited diagnostic accuracy for detecting significantly reduced myocardial perfusion. Paper IV revealed that a change in myocardial perfusion after revascularization is not associated with a change in peak oxygen uptake in patients with CCS. Finally, Paper V investigated the correlation between serum estradiol levels and myocardial perfusion in healthy women, showing that estradiol levels might influence the myocardial perfusion.

In summary, this thesis highlights different factors that influence myocardial perfusion in both patients with CCS and healthy women. The results of this thesis could contribute to improve the diagnostics of patients with CCS.

Key words
Chronic coronary syndrome, functional imaging, stress perfusion, coronary artery stenosis, sex differences

Classification system and/or index terms (if any)

Supplementary bibliographical information

Language
English

ISSN and key title
ISSN 1652-8220
Lund University, Faculty of Medicine Doctoral Dissertation
Series 2025:114

ISBN
978-91-8021-767-5

Recipient's notes

Number of pages 62

Price

Security classification

Signature

Date 2025-09-09

Determinants of myocardial perfusion

Multimodality imaging in chronic coronary syndrome

Anna Székely

LUND
UNIVERSITY

Faculty Opponent
Professor Juhani Knuuti
University of Turku

Evaluation Committee
Associate Professor Sasha Koul
Lund University

Professor Ylva Hellsten
Copenhagen University

Professor Morten Böttcher
Aarhus University

Cover illustration: Created by Noémi Székely

Faculty of Medicine, Clinical Physiology, Department of Clinical Sciences Lund, Lund University, Skåne University Hospital, Lund, Sweden

ISBN: 978-91-8021-767-5

Lund University, Faculty of Medicine Doctoral Dissertation Series 2025:114
ISSN: 1652-8220

Printed in Sweden by Media-Tryck, Lund University, Lund 2025

This thesis is dedicated to my parents, brother and sister

Előtted a küzdés, előtted a pálya,
Az erőtlen csügged, az erős megállja.
És tudod: az erő micsoda? - Akarat,
Mely előbb vagy utóbb, de borostyánt arat.

— Arany János

Contents

List of papers

This thesis is based on the following publications and manuscripts, which in the text will be referred to by their Roman numerals.

I. **Quantitative myocardial perfusion should be interpreted in the light of sex and comorbidities in patients with suspected chronic coronary syndrome: A cardiac positron emission tomography study**. A. Székely, K. Steding-Ehrenborg, D. Ryd, F. Hedeer, K. Valind, S. Akil, C. Hindorf, E. Hedström, D. Erlinge, H. Arheden, H. Engblom. *Journal of Clinical Physiology and Functional Imaging, 2024;44(1):89-99*

II. **Influence of different time framings, reconstruction algorithms and post-processing methods on the quantification of myocardial blood flow from 13 N-NH3 PET images**. S. Akil, A. Székely, F. Hedeer, B. Olsson, H. Engblom, C. Hindorf. *Journal of Clinical Physiology and Functional Imaging, 2024;44(2):154-63*

III. **Invasive coronary angiography has limited diagnostic accuracy for detecting significant reduction of myocardial perfusion assessed by cardiac magnetic resonance**. A. Székely, S. Akil, F. Hedeer, P. Kellman, M. Carlsson, D. Erlinge, H. Arheden, H. Engblom. *The American Journal of Cardiology, 2025;247:68-75*

IV. **Change in myocardial perfusion does not correlate to change in peak oxygen uptake after coronary revascularization – a positron emission tomography study**. A. Székely, S. E. Akil, H. Mosén, K. Steding-Ehrenborg, C. Hindorf, F. Hedeer, H. Arheden, H. Engblom. *Submitted*

V. **Myocardial perfusion during stress correlates with serum estradiol levels in healthy pre- and postmenopausal women**. A. Székely, K. Pola, E. Henic, P. Kellman, H. Arheden, H. Engblom. *Manuscript*

Author's contribution to the papers

	Study I	**Study II**	**Study III**	**Study IV**	**Study V**
Study design	2	2	2	3	3
Ethical application	0	0	0	0	3
Data acquisition	1	0	1	2	3
Data analysis	3	3	3	3	3
Statistical analysis	3	0	3	3	3
Figures and tables	3	1	3	3	3
Interpretation of results	3	1	3	3	3
Preparation of manuscript	3	1	3	3	3
Revision of manuscript	3	1	3	-	-
Reply to reviewers	3	1	3	-	-

Not yet applicable	-
No contribution	0
Limited contribution	1
Moderate contribution	2
Significant contribution	3

Acknowledgements

Låt oss inte älska med ord eller fraser, utan i handling och sanning

— Första Johannesbrevet 3:18

I started in the Cardiac-MR group in the summer of 2018 during medical school, and I finish my PhD in the group seven years later. I have met plenty of amazing people during these years, who have supported me and taught me things about both research, medicine and life. I hope to be able to pay everything I learned forward and continue to grow with you in my life.

Henrik and Katarina, thank you for supervising me during my PhD. Thank you Henrik for your patience, always positive attitude, believing in me and challenging my perspectives on life. Katarina, thank you for your listening, guidance and honest words.

Thank you to all my colleagues in the Cardiac-MR group. Ellen, for introducing me to the group in 2018, and always supporting and inspiring me. Håkan, for taking me in, the reflections and your honesty. Mariam, for being an amazing team mate. Shahnaz, for paving the way for this thesis with the MYOMER study, for all the fun conferences and talks. Per, for teaching me how to make great figures and all the interesting discussions. Johannes, Erik, Anthony, Barbro, Einar, Tony and Fredrik H, thank you for making me feel welcome to the group and always being available to help me with my questions. Thank you to the Medviso team for your support when I am lost in the technical jungle and for your kindness.

Anna and Annmarie, thank you for all the effort you put into making research happen, and for always being someone I could talk to, about anything. Ann-Helen, Johanna, Lotta, Christel, Klara, Abir, Beatrice, Reza and Ashwin, thank you for your patience, kindness, all the fun we have had and your willingness to walk the extra mile for research. Johan, Mikael, Henrik M, Maria, Mari, Amanda, Pia and Romeissa for your patient support in my development in the clinical work and for fruitful discussions.

Elsa and Karin, I am so thankful I did this journey with you by my side. Elsa, thank you for always having time for me, always listening and your warm heart. Karin, for you patience when working with me on projects, for your sharp questions and honesty. Tania L, thank you for those 6 months under the same roof and for all reflective talks. Anders and Petter, thank you for always being available to help out and your kindness. Kristian, Martin, Axel, Marjolein, Björn, Fanny, Jonathan, Julius and Theo, thank you for all our discussions and team work, and for making PhD life more fun. Alessandro

and Mattias, thank you for always having time for my questions and for all laughter combined with serious discussions.

I am very grateful to all patients and healthy volunteers taking time and effort to participate in our studies. You contribute to improving the future health care of patients and increasing our understanding of human physiology.

My amazing friends Amanda, Sofia, Dieuwke, Tania S, Ella, Björn, Alfred and Simon. Thank you for accepting me as I am, but also inspiring me to be the best version of myself.

My loving family, Papa, Mama, Bali and Noémi. Thank you for all the unconditional love, you mean the world to me. And lastly, my fiance David. Thank you for supporting me on this journey and for making me the happiest person in the world when I get to come home to you every day.

Abbreviations

AIF arterial input function

BSREM block-sequential regularized expectation maximization

CCS chronic coronary syndrome

CMR cardiac magnetic resonance

CPET cardiopulmonary exercise testing

CT computed tomography

ECG electrocardiogram

ECV extracellular volume

EFP early follicular phase

ICA invasive coronary angiography

LAD left anterior descending coronary artery

LCX left circumflex coronary artery

LGE late gadolinium enhancement

MLP mid-luteal phase

MPR myocardial perfusion reserve

OSEM ordered-subsets expectation maximization

PCI percutaneous coronary intervention

PET positron emission tomography

qFPP quantitative first pass perfusion

RCA right coronary artery

ToF time-of-flight

VOI volume of interest

Popular Science Summary

The heart is a muscle that constantly pumps blood to the lungs and the organs of the body. The heart muscle itself is supplied by blood through the vessels of the heart, called coronary arteries. Coronary artery disease is caused by alterations in the blood supply to the heart muscle. The blood supply of the heart muscle is called myocardial perfusion (myo=muscle, cardial=heart, perfusion=blood flow). The buildup of fat, cholesterol and other substances in the coronary arteries can lead to the development of atherosclerotic plaques, decreasing myocardial perfusion. During stable periods, coronary artery disease is referred to as chronic coronary syndrome (CCS), which is characterized by insufficient myocardial perfusion as the oxygen demand of the myocardium increases, for instance during exercise. When the blood supply to the heart muscle does not meet the metabolic needs of the tissue, ischemia develops. Ischemia can lead to symptoms such as shortness of breath and chest pain. Chest pain is one of the most common reasons for patients to seek medical attention. However, shortness of breath and chest pain can be caused by several conditions besides CCS. To assess if the symptoms are caused by ischemia of the heart muscle, patients undergo diagnostic tests such as cardiac magnetic resonance (CMR) or cardiac positron emission tomography (PET). These diagnostic tests create visual images of the myocardial perfusion. Furthermore, CMR and PET enable absolute quantification of myocardial perfusion, meaning these examinations provide numbers on how much blood reaches the heart muscle in ml/min/g. If a diagnostic test indicates that there is ischemia in the heart muscle, the patient might be referred for a procedure called invasive coronary angiography (ICA), where catheters guided by X-ray images are used to access the blood vessels of the heart. Anatomical images of the blood vessels are obtained, and the degree of narrowing of the blood vessels due to atherosclerosis is evaluated. A vessel with plaque can be opened with a stent placed by the catheters, or replaced during open heart surgery. This is referred to as revascularization.

The aim of this thesis was to investigate how different factors can affect myocardial perfusion, and to evaluate different diagnostic methods for ischemia assessment.

Paper I showed that myocardial perfusion is influenced by sex, age, hypertension, diabetes and smoking, regardless of the presence of atherosclerotic plaques in the coronary arteries.

Paper II demonstrated that myocardial perfusion values in ml/min/g obtained from PET images differ according to how the images are processed.

Paper III found that visual assessment of atherosclerosis on ICA has limitations when used to detect reduced myocardial perfusion assessed with CMR.

Paper IV revealed that change in myocardial perfusion and exercise performance after revascularization are unrelated.

Paper V investigated the relationship between estradiol levels in the blood and myocardial perfusion in healthy women, showing that at higher estradiol levels, myocardial perfusion might be lower.

This thesis highlights the different factors that influence myocardial perfusion in both patients with CCS and healthy women. The results of this thesis could contribute to improve the diagnostics of patients with CCS.

Populärvetenskaplig sammanfattning

Hjärtat är en muskel vars huvudsakliga funktion är att pumpa syresatt blod till kroppens organ och syrefattigt blod till lungorna. För att kunna genomföra detta arbete behöver hjärtmuskeln förses med syre- och näringsrikt blod. Hjärtmuskeln försörjs med blod genom blodkärl kallade kranskärl, som täcker utsidan av hjärtat och sedan grenar sig till mindre kärl i hjärtmuskeln. När hjärtat behöver jobba extra hårt, till exempel under en löptur, ökar syrebehovet i hjärtmuskeln. För att möta detta ökade syrebehov vidgar sig kranskärlen, vilket ökar blodflödet till hjärtmuskeln.

Kroniskt koronart syndrom är en vanlig diagnos som innebär att blodflödet till hjärtmuskeln inte ökar tillräckligt mycket under ansträngning för att möta syrebehovet, till exempel på grund av förträngning i kranskärlen. Syrebrist i vävnaden kallas för ischemi. Symptom på ischemi kan vara uttalad andfåddhet eller bröstsmärta vid ansträngning. Dessa symptom är dock ospecifika och kan även bero på andra bakomliggande orsaker. För att avgöra om symptomen orsakas av kroniskt koronart syndrom kan patienten genomgå olika bilddiagnostiska undersökningar av hjärtat. Två exempel på bilddiagnostiska undersökningar är magnetkameraundersökning (MR), där kroppens magnetiska egenskaper används för att avbilda organ, eller positronemissionstomografi (PET), där patienten får ett radioaktivt ämne vars strålning detekteras med en kamera. Vid hjärt-MR och hjärt-PET kan man beräkna blodflödet till olika delar av hjärtat. Om undersökningarna kombinerat med den kliniska bedömningen tyder på att patienten har kroniskt koronart syndrom, kan medicinsk behandling sättas in för att lindra patientens symptom och förbättra prognosen. I vissa fall kan patienten även genomgå koronarangiografi, där man går in med katetrar till kranskärlen genom artärerna i handleden eller ljumsken. Med röntgenstrålning avbildar man kranskärlen och kan vid behov öppna förträngningar i kranskärlen.

Syftet med denna avhandling var att undersöka vilka faktorer som kan påverka hjärtats blodförsörjning och utvärdera olika bilddiagnostiska metoder för att mäta blodflödet i hjärtmuskeln.

Studie I visade att hjärtats blodförsörjning påverkas av kön, ålder, högt blodtryck, diabetes och rökning oberoende av om kranskärlen har förträngningar.

Studie II presenterade skillnader i uppmätt blodflöde i hjärtmuskeln beroende på hur hjärt-PET bilderna har skapats och analyserats.

Studie III demonstrerade att visuell bedömning av förträngningar i kranskärlen på koronarangiografi har begränsad förmåga att påvisa nedsatt blodflöde i hjärtmuskeln.

Studie IV visade att det inte finns något samband mellan förändring av blodflödet i hjärtmuskeln och förändring av träningskapacitet efter öppnandet av kranskärlen.

Studie V undersökte sambandet mellan östrogennivåer i blodet och blodflödet i hjärtmuskeln hos friska kvinnor, och visade att blodflödet kan vara lägre vid högre östrogennivåer.

Sammanfattningsvis belyser denna avhandling olika patientspecifika och metodologiska parametrar som påverkar det uppmätta blodflödet i hjärtmuskeln. Resultaten kan hjälpa till att förbättra diagnostiken av patienter med kroniskt koronart syndrom.

Chapter 1

Introduction

The main function of the heart is to deliver oxygenated blood to the organs of the body and deoxygenated blood to the lungs. Cardiac muscle cells (myocytes) contract and relax and thereby pump the deoxygenated blood from the right ventricle, through the pulmonary artery, to the lungs. The oxygenated blood returns to the left atrium of the heart through the pulmonary veins, continues to the left ventricle and is pumped through the aorta to the systemic circulation, delivering oxygen to all organs. The deoxygenated blood returns through the venae cavae to the right atrium and continues to the right ventricle (Figure 1.1). The cardiac muscle is under a constant workload, in need of its own oxygen supply. The arteries supplying the cardiac muscle with blood are named coronary arteries.

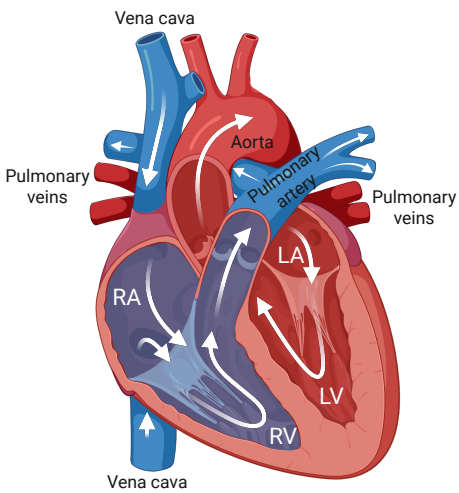

FIGURE 1.1: Overview of the anatomy and blood circulation of the heart and proximal vessels. *RA = right atrium, RV = right ventricle, LA = left atrium, LV = left ventricle. Created in BioRender. Szekely, A. (2025) https://BioRender.com/s4x92re*

1.1 Coronary anatomy and function

There are three main coronary arteries: the left anterior descending coronary artery (LAD), left circumflex coronary artery (LCX) and right coronary artery (RCA) (Figure 1.2). The main coronary arteries arise from the sinus valsalva of the aortic root and run on the epicardial (outer) surface of the heart, hence referred to as epicardial coronary arteries. The LAD and LCX both emerge from the left main artery of the left aortic sinus, and the RCA emerges from the right aortic sinus. At rest, 5-4% of the cardiac output (total blood volume ejected by the left ventricle in one minute) goes to the coronary arteries. The epicardial coronary arteries branch into arterioles which continue into a dense network of capillary beds through the myocardial wall towards the endocardial (inner) surface of the heart. Hence, the myocardium is supplied from the "outside" (the epicardium) to the "inside" (the endocardium). The metabolic demand of the myocardium depends on the workload of the heart. At rest, the myocardium extracts 70-80% of the oxygen supplied by the blood through the coronary arteries. This is the highest oxygen consumption at rest by any organ of the body. However, when workload increases, for instance during exercise, the oxygen supply needs to be increased as well to meet the metabolic demands of the myocardium. Since the extraction rate of oxygen from blood is already near maximized, the increased oxygen demand can only be met by increasing the perfusion of the myocardium. This is done by regulating the coronary vascular resistance, through vasodilation of the vessels[1,2].

Vasodilation of a vessel increases the radius of the vessel, in turn decreasing the resistance according to Poiseuille's law:

$$R = \frac{8L\eta}{\pi r^4}$$

(R = resistance, L = length of the vessel, η= viscosity of blood, r = radius of the vessel)

The decreased resistance increases the flow through the vessel, according to Ohm's law:

$$Q = \frac{\Delta P}{R}$$

(Q = flow, ΔP = difference in pressure, R = resistance)

The coronary vascular resistance is mainly modulated by vasodilation of the arterioles. Increasing the blood flow through the microvasculature when the arterioles vasodilate leads to further vasodilation of the prearterioles and epicardial coronary arteries (Figure 1.3).

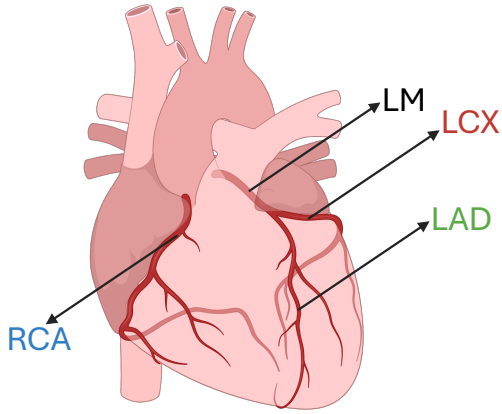

FIGURE 1.2: Overview of the epicardial arteries of the heart. *Created in BioRender. Szekely, A. (2025) https://BioRender.com/7lwaz9p*

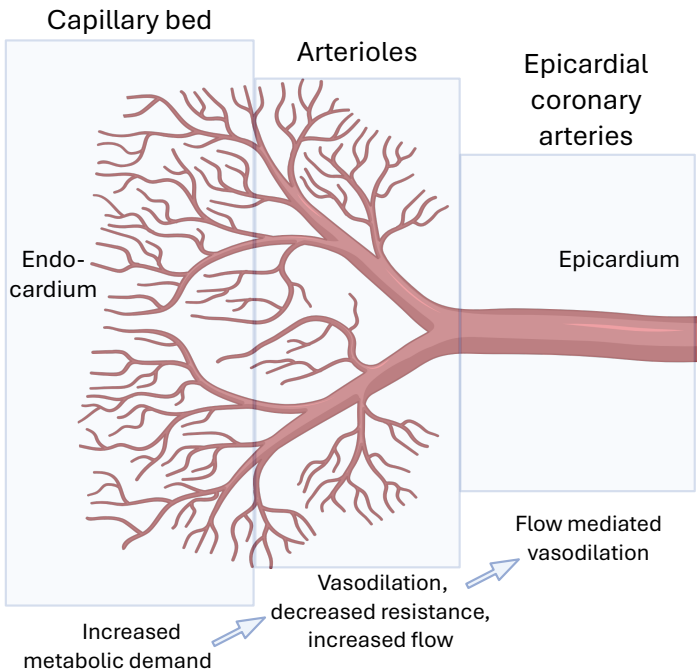

FIGURE 1.3: An overview of the vascular bed of the myocardium. The epicardial coronary arteries branch into smaller vessels from the epicardium through the myocardium to the endocardium. Increased metabolic demand in the myocardium initiates vasodilation of the arterioles, decreasing the resistance and increasing the blood flow, leading to further vasodilation of the large arteries. *Created in BioRender. Szekely, A. (2025) https://BioRender.com/3zq62o8*

1.2 Chronic coronary syndromes

Cardiovascular disease is the leading cause of death worldwide[3]. Coronary artery disease refers to conditions that reduce perfusion of the myocardium and can be divided into an acute phase and a stable phase. In its stable form, coronary artery disease is called chronic coronary syndrome (CCS), which includes functional and/or structural alterations of the large arteries and microcirculation of the heart, leading to transient ischemia of the myocardium, usually triggered by physical or emotional stress[4].

Pathophysiology of CCS

Previous focus of the pathophysiology of CCS has mainly been on epicardial coronary arteries and focal, flow-limiting stenoses. If the radius of an artery is compromised by a stenotic lesion, the resistance will increase and the blood flow will decrease according to Poiseuille's and Ohm's law (Figure 1.4). This can usually be compensated for during rest through vasodilation. However, when the oxygen demand increases during physical activity, a vessel with a significant stenosis is already maximally vasodilated and not able to increase its radius. Therefore, the blood flow through the artery may not be able to meet the metabolic demand of the tissue.

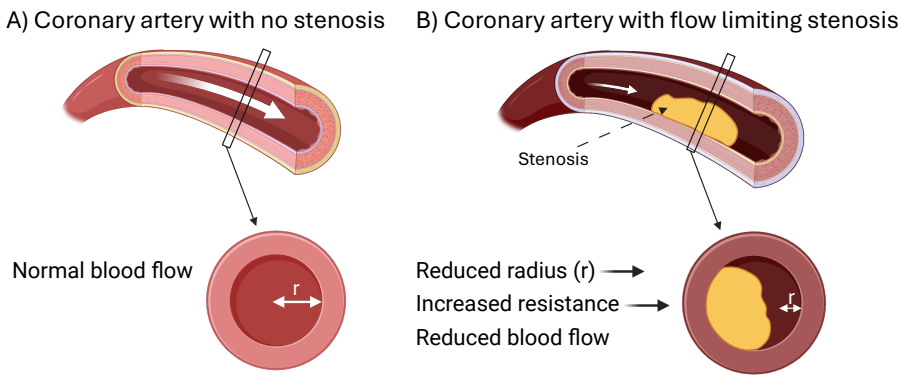

FIGURE 1.4: A) shows a coronary artery with no stenosis and normal blood flow. B) shows a coronary artery with a flow limiting stenosis, reducing the blood flow according to Poiseuille's and Ohm's law. *Created in BioRender. Szekely, A. (2025) https://BioRender.com/8nxvbsf*

However, the understanding of the pathophysiology of CCS has evolved from a simple to a more complex model over the years. Epicardial disease in the coronary arteries can be either structural, such as focal or diffuse atherosclerosis, or functional, such as temporary vasospasm. Alterations of the microvasculature, referred to as microvascular dysfunction, is another pathophysiological mechanism behind CCS. The alterations of the microvasculature can also be structural, such as remodeling of the arterioles or intravascular fibrosis, and functional due to endothelial dysfunction. The alterations in the vasculature are predisposed by several known risk factors, such as hypertension, dyslipidemia, smoking and increasing age[4].

Regardless of if the ischemia is caused by alterations in the macro- or microcirculation, or caused by extra-cardial factors such as blood pressure drop or anemia, they all have in common that they induce ischemia due to an inability to meet the oxygen demand of the myocardium[4]. The consequences of ischemia occurs in several steps, often referred to as the ischemic cascade. The ischemia induced in the myocardium impairs first the relaxation of the myocardium (diastolic function) and then the contraction of the myocardium (systolic function), since the relaxation during diastole requires a higher energy consumption. During these phases, the ischemia is often not recognized clinically and is referred to as silent ischemia. This is followed by electrocardiographic (ECG) changes, and lastly the onset of symptoms such as chest pain (angina) or shortness of breath (dyspnea)[5].

Clinical presentation and evaluation of CCS

For proper clinical evaluation of a patient with suspected CCS, the clinical presentation needs to be integrated with the available diagnostic tools. The *2024 ESC Guidelines for the management of chronic coronary syndromes*[4] is one of the latest guidelines for the diagnostic process of patients with suspected CCS. An important corner stone in the diagnostic process is the understanding of *choosing wisely*, aiming to provide the correct diagnostic tool for the individual patient, avoiding unnecessary examinations while providing the correct diagnosis.

To evaluate a patient with suspected CCS it is important to assess if the symptoms are caused by ischemia of the myocardium or by another condition, and if the symptoms are stable or acute. Angina and dyspnea are the two most common symptoms caused by CCS, however sex, age and comorbidities can affect the presentation of these symptoms. The symptoms are usually triggered by physical or mental stress and relieved at rest. Change in symptomatology over a short period of time, or symptoms present already at rest can, indicate unstable angina, requiring acute care. Furthermore, risk factors of CCS need to be considered - for instance smoking, dyslipidemia, hypertension, diabetes and heredity all increase the probability that the patient has developed CCS. Some commonly available tools to further understand the etiology of the patient's symptoms are blood pressure measurement, ECG assessment, heart and lung auscultation, palpation of the area of pain, and blood samples. The information from the initial examination enables an evaluation of the pre-test clinical likelihood of CCS, based on symptom characteristics, risk factors, age and sex. Very low clinical likelihood does usually not require any further testing. At low to moderate likelihood, computed tomography (CT) angiography is recommended, which is an anatomical imaging tool depicting the anatomy of the coronary vessels and the presence of atherosclerosis in the coronary arteries. Furthermore, at moderate to high likelihood of CCS, functional imaging modalities are recommended, such as single photon emission computed tomography, photon emission tomography (PET), cardiac magnetic resonance (CMR) and echocardiography. The choice of modality should be based on local expertise, availability and the information required to be obtained from the examination. Table 1.1 shows a comparison of imaging modalities used for evaluation of CCS. At very high clinical likelihood, the patient should be referred for invasive coronary angiography (ICA) with the possibility of revascularization[4,6].

TABLE 1.1: General overview and comparison of imaging modalities used clinically for evaluation of the coronary arteries and myocardial perfusion according to the guidelines for CCS [4].

	CTA	PET	SPECT	CMR	Echocardiography	ICA
Clinical likelihood	low-moderate	moderate-high	moderate-high	moderate-high	moderate-high	very high
Anatomical	yes	no	no	no	no	yes
Functional	no	yes	yes	yes	yes	yes (iFR, FFR, iMR)
Quantitative perfusion	no	yes	no	yes (limited)	no	no
Ionizing radiation	yes	yes	yes	no	no	yes
Invasive	no	no	no	no	no	yes
User dependent	no	no	no	no	yes	yes

CTA = computed tomography angiography, PET = positron emission tomography, SPECT = single photon emission computed tomography, CMR = cardiac magnetic resonance, ICA = invasive coronary angiography, iFR = instantaneous wave-free ratio , FFR = fractional flow reserve, iMR = index of microvascular resistance.

The coronary angiogram might depict a coronary artery stenosis without any significant effect on perfusion downstream of the lesion [7]. Likewise, a patient can present with a normal angiogram but still suffer from ischemia due to non-obstructive coronary artery disease. According to the most recent SWEDEHEART report, half of ICAs performed on women aged 60-69 years show no significant coronary artery stenosis [8]. Therefore, functional evaluation of myocardial perfusion can add significant diagnostic information, and has become an important diagnostic tool to avoid unnecessary invasive interventions, reducing patient risk [4].

Treatment of CCS

Lifestyle changes such as smoking cessation, increased physical activity and improved diet should be recommended to all patients suffering from CCS. The development of pharmacological treatment options have improved survival and quality of life for patients suffering from cardiovascular diseases [8]. They include anti-anginal drugs like beta-blockers, calcium-channel blockers and nitrates, anti-trombotic drugs like aspirin and clopidogrel, blood pressure- and lipid-lowering drugs like angiotensin-converting enzyme inhibitors and statins and glucose lowering SGLT2 inhibitors. This growing collection of treatments enables patient-specific treatment depending on the presentation of the disease, comorbidities and tolerance [4]. If medical therapy does not improve the symptoms of patients with obstructive coronary artery disease, invasive coronary angiography with revascularization can be considered. Coronary artery bypass graft surgery can be indicated if the patient has significant stenoses in all three main coronary arteries, referred to as 3-vessel disease, or significant proximal left sided stenosis. During this surgical procedure, healthy vessels from other parts of the body are grafted to the coronaries, bypassing the obstructions [9].

Sex differences in CCS

Women are underrepresented within cardiovascular research and are under-diagnosed and under-treated for cardiovascular diseases[10]. There are several sex differences in the development and presentation of coronary artery disease. Women develop coronary artery disease 10 years later than men[11]. After menopause, the risk of developing cardiovascular diseases increases[10]. Women more often present with non-obstructive coronary artery disease than men[12], and approximately half of the women presenting with angina have microvascular dysfunction[13]. Furthermore, women have higher myocardial perfusion at stress than men[14] and sex-specific normal values for myocardial perfusion have been proposed[15], but this is currently not implemented in clinical practice. Estrogen has been shown to have cardioprotective effects, and differences in sex hormone levels might partly explain the sex differences in cardiovascular diseases[16]. Hormone replacement therapy has been shown to improve anginal symptoms in post-menopausal women[17]. A previous study has shown that hormone replacement therapy increases myocardial perfusion reserve in women with angina[18]. Furthermore, pre-menopausal women undergo cyclic variations in sex hormone levels during their menstrual cycle, with low sex hormone levels during the early follicular phase (EFP) and high estrogen and progesterone levels during the mid-luteal phase (MLP). Previous studies have shown that resting heart rate[19], sympathetic activity[20] and coronary flow velocity reserve[21] increase in the MLP. However, due to the practical challenges of investigating cardiac function during different phases of the menstrual cycle[22], more comprehensive studies are lacking. Increased knowledge of the coronary physiology in women in relation to sex hormone levels has the potential to contribute to a more equal and individualized health care and to improve the clinical evaluation of women with CCS.

1.3 Positron Emission Tomography (PET)

Positron emission tomography is a nuclear imaging modality depicting the physiology of the human body using radiopharmaceuticals - tracer molecules with radionuclide emitting positrons. Different organs and processes can be visualized and quantified using PET, including myocardial perfusion. PET is today considered to be the gold standard for myocardial perfusion quantification [23] and has shown high sensitivity and specificity to rule in or rule out functionally significant coronary artery stenoses [24].

Physics of PET imaging

The radionuclide has an unstable nucleus, with an excess number of neutrons or protons leading to an abundance of energy. The nucleus aims to reach a stable, less energetic state by changing its composition, i.e by undergoing a radioactive decay.

In PET, the nuclide usually has an excess of protons. The nuclide therefore transforms a proton into a neutron through decay. This transformation mediates a positron and a neutrino. The positron moves through the matter, until it loses enough of its kinetic energy to annihilate with an electron. At this annihilation process, two annihilation photons emerge. These photons travel in opposite directions of 180 degrees with an energy of 511 keV. Photon detectors at opposite sides capture the annihilated photons at the same time - this is referred to as *coincidence*. Since the photons travel with the exact same speed, the position of the annihilation can be located (Figure 1.5) [25]. Between the annihilation process and the detection, *Compton scatter* occurs due to the interaction of the photons with electrons of the human tissue. This interaction changes the direction of the photons, and decreases their energy. Depending on the distance between the emitting tissue and the detector as well as the density of electrons in the tissue, the number of photons reaching the detector without interaction with the tissue decreases exponentially, leading to attenuation [26]. The number of decays per second is referred to as the activity of the radionuclide. The activity decreases over time, and is conventionally measured in Becquerel, Bq. The half-life of a PET radionuclide depends partly on its activity, which in turn depends on the number of undecayed nuclei present. The half-life also depends on the biological elimination of the radionuclide from the human body [25]. The half-life of the radiopharmaceuticals used in clinical practice is an important parameter to consider for logistical reasons, as well as for radiation exposure. Therefore, the choice of radiopharmaceutical plays an important role in clinical examinations.

Radiopharmaceuticals

Several radiopharmaceuticals with different properties are available for myocardial perfusion imaging, including ^{15}O water, ^{82}Rb, ^{18}F flurpiridaz and ^{13}N ammonia [27]. Pharmaceuticals with a short half-life, such as ^{15}O water which has a half-life of less than two minutes, require on-site cyclotrons. Furthermore, the extraction fraction of the radiopharmaceutical, i.e. the fraction of the radiopharmaceutical extracted into the myocardium from the blood, plays an important role in the perfusion quantification. ^{15}O water PET is considered the reference method for perfusion quantification due to its free diffusibility into the myocardium, providing a linear relationship of 1:1 between

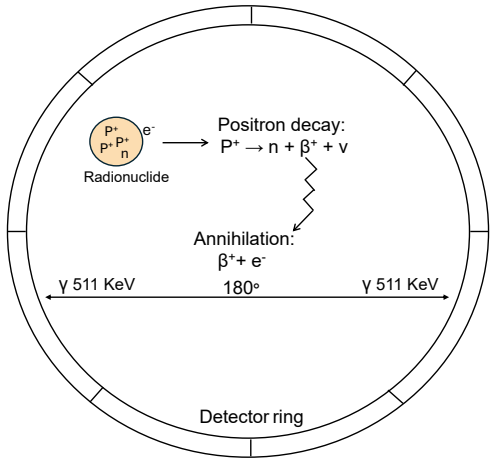

FIGURE 1.5: The physics behind PET imaging. From the radionuclide transforming a proton (P^+) to a neutron (n), a positron (β^+) and a neutrino (v), to the annihilation of the positron with an electron (e^-), converting their mass to energy of a photon (γ), partly decreased by Compton scatter before reaching the photon detector ring surrounding the patient.

signal intensity and myocardial blood flow, or a 100% extraction fraction [28]. Due to the short half-life and free distribution of ^{15}O water, the images produced have low counts, and are mostly used for absolute perfusion quantification rather than qualitative visual evaluation of images [25]. The current thesis uses ^{13}N ammonia which has a half-life of almost 10 minutes [28]. However, the extraction fraction for ^{13}N ammonia is around 80%. Hence, the higher perfusion, the more it diverges from ^{13}N ammonia uptake [27]. However, ^{13}N ammonia rapidly clears from blood, and therefore provides quality images for visual interpretation [25]. Furthermore, ^{13}N ammonia has a shorter positron range than ^{15}O water, improving image resolution [27]. The radiation dose of a ^{13}N ammonia PET examination is 4 mSv including both the rest and stress examination, and the radiation of the integrated CT examination [29].

Image acquisition

The photon detectors are located around the patient and usually consist of scintillation crystals, where the annihilated photons reaching the detectors interact with the crystals. These scintillated photons are then detected by photonmultiplier tubes, where the photon energy is used to create electrical currents [26]. List mode acquisition is a data acquisition technique where detailed information of each detected event of coincidence is recorded and saved separately. This allows flexible image reconstruction and analysis after image acquisition [30]. After acquisition, the data collected by the detectors are organized in so called sinograms, based on calculations of the line of response, i.e. the line between the annihilation and the detection of the photons [26]. Time-of-flight (ToF) is a reconstruction method that improves the localization of the annihilation from the line of response [31, 32], increasing image quality [33]. As mentioned above, attenuation occurs

due to scatter. Attenuation correction is usually conducted with an integrated CT[25]. Ordered-subsets expectation maximization (OSEM) is the processing method for image reconstruction used in the current thesis[26]. Time-frame schemes are used to determine how the PET data should be segmented over time to reconstruct dynamic PET images.

Myocardial perfusion quantification

Myocardium with high uptake of the radiopharmaceutical is considered to have a higher perfusion than myocardium with low uptake. Dynamic image acquisition enables myocardial perfusion quantification. The activity concentrations as a function of time in the left ventricular blood pool and myocardium are derived from the dynamic PET images, creating time-activity curves (Figure 1.6). The temporal resolution of the time-activity curves can be affected by choice of time-frame schemes. Furthermore, the time-activity curve for the ventricular blood pool might be affected by different degree of partial volume effects and spill in and spill out of activity, depending on the anatomical location of the volume of interest (VOI) in the blood pool[34]. The exchange of activity between the blood pool and the myocardium is described using a compartment model. In the compartment model, rate constants are used to represent the transportation of the radiopharmaceutical between the different compartments in the model (Figure 1.6)[35]. The deGrado[36] and Krivokapich[37] are two-compartment models (arterial blood pool compartment and tissue compartment). Hutchins is a three-compartment model (arterial blood compartment, interstitial and intracellular space compartment). Hence, the tissue compartment is divided into two separate compartments in the Hutchins model[38]. Different number of compartments and algorithms used in the mentioned compartment models might affect the perfusion quantification[39].

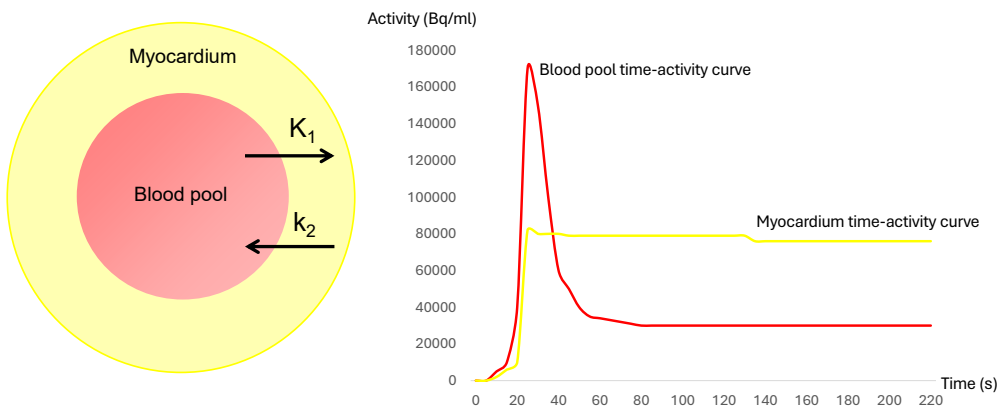

FIGURE 1.6: Left: A schematic figure of the two rate constants K_1 (transportation of radiopharmaceutical from blood pool to myocardium) and k_2 (transportation of the radiopharmaceutical from the myocardium to the blood pool) used in two-compartment models. In three-compartment models, the myocardium is divided into an interstitial and an intracellular compartment and the rate constants for these compartments are added to the model. Right: A schematic graph showing the time-activity curve in the blood pool and myocardium used as input information for the compartment models providing absolute perfusion values.

1.4 Cardiac Magnetic Resonance (CMR)

Magnetic resonance imaging was developed for clinical use during the 20th century, and today it is a widely-used imaging technique with a large array of clinical applications [40]. Recent developments have enabled the use of magnetic resonance imaging for myocardial perfusion quantification [41].

Physics of CMR

Just like in PET, protons play an important role in CMR. However, in CMR it is the magnetic properties of the protons of the body that create detectable signals used to reconstruct images. Therefore, CMR has the advantage of being an examination free of ionizing radiation.

Protons are positively charged and spin around an axis, creating an electric current that generates a magnetic field. When these protons experience an external magnetic field, B_0, they create a net magnetization vector (M) parallel with B_0. The net magnetization M in space can be divided into the magnetization in the longitudinal (z) and transversal (xy) plane. M in the direction of B_0 is referred to as M_z and represents the longitudinal direction (Figure 1.7). Furthermore, the protons rotate around the direction of B_0, so called precession, in the transversal plane. The frequency of the precession is decided by the external magnetic field B and the gyromagnetic properties of the proton (γ) according to the Larmor equation:

$$Larmor\ frequency = \gamma \times B$$

M_{xy} is the magnetization in the transversal plane. In the presence of a single magnetic field B_0, the precession of the protons is distributed evenly in the xy-plane, hence M_{xy} is zero [40, 42]. The strength of the magnetic field is measured in tesla (T). In the current thesis, the external magnetic field, B_0, of the MR scanner is 1.5T, which is often used for cardiac imaging [43].

To create a signal, the direction of the net magnetization vector needs to be changed, or flipped, from the z-direction towards the xy-plane. This is done by applying a radiofrequency pulse, which is a magnetic field that oscillates at the Larmor frequency, called B_1. The protons pick up energy from the radiofrequency pulse when they have the same same frequency as B_1, hence the name "magnetic resonance". The protons start to precess around B_1 and this flips the net magnetization from the z-direction towards the xy-plane (Figure 1.7). However, the B_1 component is only temporary, and the net magnetization recovers towards the z-plane. During this recovery, the precession of the net magnetization around B_0 induces a voltage in the receiver coils. T_1 is the longitudinal relaxation time in milliseconds for M_z to return to 63% of its original value in the z-plane. T_2 refers to the transversal relaxation time for M_{xy} to decay to 37% of its maximal value [40, 42]. To be able to differentiate spatial localizations of the protons, the magnetic field temporarily needs to have different strengths at different parts of the cross section of the body examined. This is done by using magnetic fields changing over space, called gradients. The frequency of the precession of the protons is dependent of the magnetic field strength according to the Larmor equation. Hence, the difference in field strength caused by the gradients provides MR signals from different parts of the body with different frequencies [40].

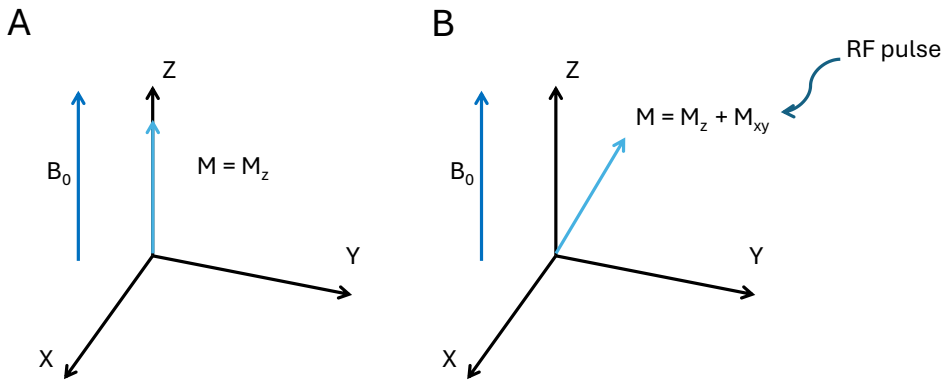

FIGURE 1.7: A simplified schematic figure of the net magnetization M in the magnetic field. A) In the external magnetic field B_0 the net magnetization is aligned with the longitudinal direction, M_z. B) When an RF pulse (radiofrequency pulse) is applied on the magnetic field, the net magnetization flips towards the transversal direction. The net magnetization M then consists of the sum of M_z and M_{xy}.

The T_1 and T_2 time are affected by the tissue composition of the body. Water has a long T_1 time, while fat has a shorter T_1 time. The T_2 time depends on inhomogeneities in the magnetic field. Larger molecules move more slowly, creating larger inhomogeneities in the magnetic field, shortening the T_2 time, while in water the T_2 time is longer[42].

Contrast agents can be used to enhance contrast in CMR images. The most common MR contrast agents are gadolinium-based, which shortens the T_1 time. Hence, tissue with high gadolinium concentration appears brighter on T_1 weighted post-contrast images[40]. Since gadolinium is an extra-cellular contrast agent, it reaches a steady-state in the extracellular space after injection of the bolus. Late gadolinium enhancement (LGE) images can for instance be used for assessment of extracellular volume (ECV) of the myocardium and myocardial fibrosis[44, 45, 46]. The first passage of the gadolinium bolus can be used to assess myocardial perfusion.

Quantitative first pass perfusion imaging

Quantitative first pass perfusion (qFPP) CMR is a new imaging technique that has been validated against cardiac PET[41]. Since qFPP CMR enables the absolute quantification of the perfusion of the myocardium, it can be used to detect functionally significant coronary artery stenoses as well as balanced 3-vessel disease and microvascular dysfunction[47].

Myocardial perfusion is quantified using a gradient echo sequence to acquire the first pass of the gadolinium contrast agent from the veins to the arterial blood pool and further to the myocardium. Myocardium perfused by non-obstructed arteries will be reached by more gadolinium at the first passage than myocardium perfused by obstructed arteries. As mentioned above, gadolinium shortens T_1, hence tissue with high gadolinium concentration will have a higher signal intensity in T_1 weighted images.

However, the linear relationship between acquired signal intensity and gadolinium concentration decreases with increasing gadolinium concentration. The arterial input function (AIF) drives the delivery of the contrast agent to the myocardium and needs to be assessed when quantifying myocardial perfusion. However, since there is a high concentration of gadolinium in the atrial blood pool after bolus injection, the non-linearity to signal intensity will be pronounced when assessing AIF. This non-linear relationship needs to be corrected to avoid bias[48]. This can be solved by the dual sequence approach, where separate sequences are used to optimize the image for the AIF and the myocardium. ECG triggering is used during image acquisition. The ECG's R-wave triggers the acquisition of a low-resolution image in the basal short axis, from which the AIF is measured. Then, multi-slice high-resolution myocardial images are collected[49]. Myocardial images are acquired every or every other second RR-interval. If three slices are acquired (usually apical, midventricular and basal short axis slices), the myocardial high-resolution images can be acquired every RR-interval. However, if more slices are to be added (usually 2-, 3- and 4-chamber long axis slices; Figure 1.8), the short axis slices need to be acquired every other RR-interval, in-between the long axis slice acquisition, since the acquisition time of one RR-interval isn't enough to collect 6 slices. Image acquisition takes 60-120 heart beats and is acquired during free breathing with motion correction[50].

The images are reconstructed using the Gadgetron software[51]. Myocardial perfusion (in ml/min/g) is quantified at each image pixel using a two-compartment blood-tissue exchange model. This model assesses the transport of gadolinium from the blood into the myocardium through the endothelium[49, 52].

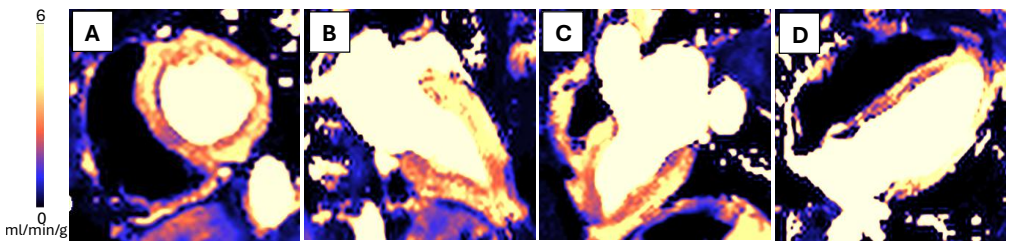

FIGURE 1.8: Quantitative perfusion maps acquired in a short axis view (A), 2-chamber view (B), 3-chamber view (C) and 4-chamber view (D) during adenosine stress.

1.5 Adenosine

Adenosine is one of the most widely-used vasodilators for stress perfusion examinations. It is a safe and well-tolerated drug, with a short half-life and few side effects. Typical side effects of adenosine include flush, dyspnea and chest pain[53]. Adenosine induces coronary vasodilation, which causes hyperemia in the myocardium. Furthermore, adenosine causes peripheral vasodilation, decreasing the blood pressure, with a secondary increase in heart rate. According to current clinical guidelines, adenosine should be administrated at a dose of 140 µg/kg/min. If heart rate does not increase by 10 beats/min or blood pressure does not decrease by 10 mmHg, the dose can be increased up to 210 µg/kg/min[43]. A recent study demonstrated that an adenosine dose of 210 µg/kg/min significantly increased the myocardial perfusion in patients with reduced ejection fraction when compared to the standard dose of 140 µg/kg/min[54].

Caffeine is an adenosine receptor antagonist, decreasing the effects of adenosine. Myocardial perfusion during adenosine stress increases after 24 hours of caffeine abstinence, when compared with 12 hours of abstinence, on a group level. However, there is a great variation on an individual level, with some patients not being affected by caffeine intake. This suggests a variation of caffeine metabolism among patients[55]. The effect of caffeine can be overcome by increasing the adenosine dose[56].

Inadequate adenosine response poses an important clinical challenge. Up to 16% of patients examined with adenosine do not achieve an adequate hyperemic response, and there is a cyclic variation of the response during adenosine infusion[57]. Using imaging modalities depicting the relative perfusion distribution, the absence of hyperemic effect on the myocardium can mask regional perfusion defects, leading to false-negative examinations. Using qFPP CMR enables the assessment of splenic switch-off. Adenosine induces vasoconstriction of the spleen, hence the signal intensity of the spleen decreases with adequate adenosine effect. Furthermore, the absence of hyperemic response leads to globally low absolute perfusion values, which can be interpreted as balanced 3-vessel disease or microvascular dysfunction, but can also be an indicator of absence of adenosine effect, especially when present with the splenic switch-off sign[58, 59]. Figure 1.9 shows a patient case from our department where inadequate adenosine effect was suspected. A 62-year-old woman underwent qFPP CMR due to dyspnea. The evening before the examination, she had a cup of coffee. Global rest perfusion was 0.9 ml/min/g and the ejection fraction 40%. The adenosine dose was increased from 140 to 170 µg/kg/min due to no heart rate increase, no blood pressure drop, and no symptoms. At 170 µg/kg/min, heart rate increased by 17 beats/minute and the patient experienced adenosine-related symptoms. Due to globally reduced myocardial perfusion (1.2ml/min/g) and no splenic switch off, absence of adenosine effect was suspected. A new stress acquisition was performed in the same imaging session with an adenosine dose of 210 µg/kg/min, showing normal global myocardial perfusion of 3.0 ml/min/g without regional ischemia. Hence the patient report could free the patient from 3-vessel disease and microvascular dysfunction. This patient case emphasizes the importance of adequate adenosine effect on hyperemia to ensure correct diagnosis.

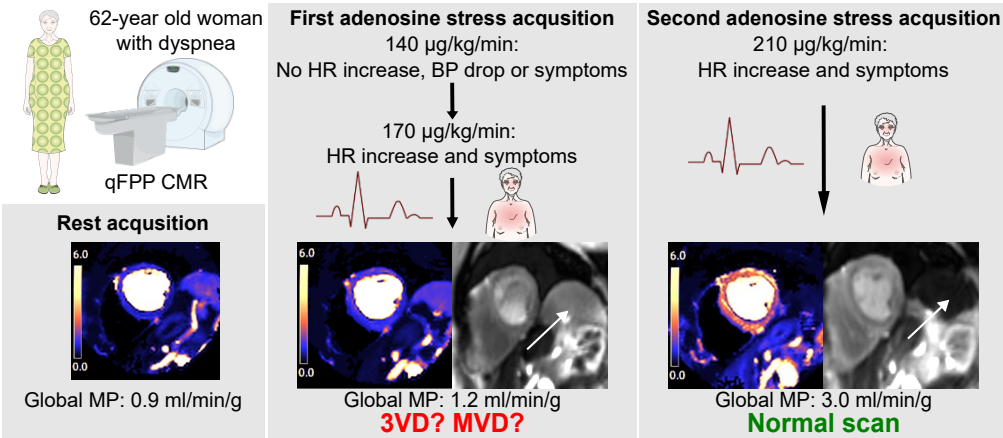

FIGURE 1.9: Visual summary of the patient case described in the main text with the three acquired myocardial perfusion maps and splenic switch off. Left; global rest perfusion of 0.9 ml/min/g. Middle; first stress acquisition with an adenosine dose of 170 µg/kg/min showing a global stress perfusion of 1.2 ml/min/g. The white arrow indicates absence of splenic switch off during this acquisition. Right; second stress acquisition with an adenosine dose of 210 µg/kg/min showing a global stress perfusion of 3.0 ml/min/g. The white arrow indicates presence of splenic switch off. *BP = blood pressure; CMR = cardiac magnetic resonance; EF = ejection fraction; HR = heart rate; MP = myocardial perfusion; MVD = microvascular dysfunction; VD = vessel disease; qFPP = quantitative first pass perfusion*

1.6 Invasive coronary angiography (ICA)

Invasive coronary angiography is an imaging modality that invasively depicts the coronary anatomy, and was first introduced in the 1960s by Dr Mason Sones. Performed under local anesthesia, the procedure involves guiding a catheter through the radial or femoral artery to the coronary arteries. Contrast agent is used to visualize the arteries via X-ray imaging. During the examination, stenotic lesions can be revascularized using stents, referred to as percutaneous coronary intervention (PCI). The most common complication is bleeding at the access site. This risk increases when the femoral artery is used, or during PCI where more anticoagulants are administered [60]. Furthermore, the rate of death, stroke or myocardial infarction associated with the procedure is around 0.1-0.2%. According to guidelines, elective invasive coronary angiography should be conducted in patients if the clinical likelihood of CCS is very high, if medical treatment only does not improve patient symptoms or if extensive obstructive coronary artery stenoses are suspected based on functional assessment of the left ventricle [4]. Degree of coronary artery stenosis can be assessed visually from the coronary angiogram as luminal diameter narrowing in %. However, the visual assessment of degree of stenosis does not reveal any information about the functional significance of the obstruction on downstream perfusion [7]. Recent developments have enabled functional assessment of coronary artery stenoses and the microvasculature, which has improved the diagnostic value of ICA. Fractional flow reserve measures the pressure drop over a coronary artery stenosis during hyperemia (induced by adenosine, for example) by dividing the pressure distal to the stenosis with the aortic pressure. Instantaneous wave-free ratio measures the same pressure gradient, but without induced hyperemia, by timing the measurement to diastole when the microvascular resistance is low. Microvascular function can be assessed quantitatively using index of microcirculatory resistance and is not affected by stenoses of the coronary arteries. It is calculated as distal pressure multiplied by the mean transit time of a bolus saline through the microvasculature during hyperemia (Figure 1.10) [61].

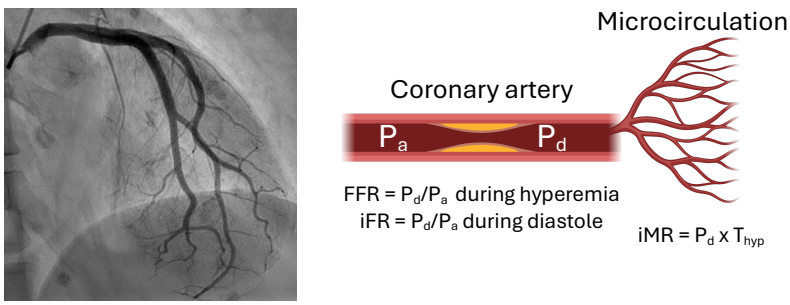

FIGURE 1.10: A coronary angiogram (left) and a schematic image of pressure measurements over the cardiac vasculature when a coronary artery stenosis is present (right). *FFR = fractional flow reserve, iFR = instantaneous wave-free ratio, iMR = index of microvascular resistance, P_a = aortic pressure, P_d = pressure distal to the stenosis, T_{hyp} = mean transit time through the microvasculature. Created in BioRender. Szekely, A. (2025) https://BioRender.com/zbjc51y*

1.7 Cardiopulmonary exercise testing (CPET)

Cardiopulmonary exercise testing provides an integrated evaluation of the cardiopulmonary system. The examination combines ECG and gas exchange assessment at rest, during and after exercise, and guides diagnostics and prognostics of patients with pulmonary and/or cardiac diseases[62].

Gas exchange physiology

Exercise performance depends on the ability to transport oxygen (O_2) to the muscles and remove carbon dioxide (CO_2) from the muscles. The cardiovascular system transports blood between the lungs and the organs, where capillary gas exchange of O_2 and CO_2 takes place. The pulmonary system ventilates air in and out of the body through the lungs, where O_2 in the alveoli is exchanged with CO_2 in the capillaries.

Oxygen uptake (VO_2) depends on cardiac function and gas exchange in the tissue, explained by the simplified Fick equation:

$$VO_2 = Q \cdot (C_aO_2 - C_vO_2)$$

(Q = cardiac output, C_aO_2 = arterial oxygen content, C_vO_2 = venous oxygen content)

During exercise, VO_2 increases by increased cardiac output and higher extraction rate of oxygen in the muscles. Furthermore, the vessels supplying the working muscles and the lungs vasodilate, increasing the blood flow to the tissue. Ventilation of the lungs also increases, matching the increased perfusion of the lungs. Hence, gas exchange depends on several mechanisms that can be evaluated using CPET.

Examination procedure and interpretation

During CPET, exercise is usually performed on a treadmill or cycle ergometer with simultaneous assessment of ECG-reaction including pulse reaction, blood pressure reaction, work capacity and exercise-provoked symptoms. A face mask or mouth piece is used to collect breathing gases, to measure O_2 uptake, CO_2 output and ventilation rate[63].

The highest volume of oxygen the body uses during exercise is termed VO_2 peak and is measured in L/min. Since body weight significantly affects exercise performance, VO_2 peak is often normalized to weight and presented as ml/kg/min. Furthermore, sex, height and age also affect exercise performance, which can be normalized for using VO_2 peak % of predicted value[64].

Both exercise capacity and myocardial perfusion have been shown to improve after cardiac rehabilitation in post-infarction patients[65]. The prognosis for patients with CCS is related to exercise capacity[66, 67, 68] and VO_2 peak is associated with myocardial perfusion in patients with aortic stenosis[69], diabetes[70] and dilated cardiomyopathy[71].

Chapter 2

Aims

The overall aim of this thesis was to increase our understanding of the determinants of myocardial perfusion using different imaging modalities, to improve diagnostics of patients with CCS. The specific aims of the studies included in this thesis were to:

Paper I Investigate to what extent sex, age, hypertension, diabetes and smoking affect myocardial perfusion assessed with ^{13}N ammonia PET independent of degree of coronary artery stenosis, in patients with suspected CCS.

Paper II Examine to what extent the quantification of myocardial perfusion from dynamic ^{13}N ammonia PET images is affected by different time-frame schemes, reconstruction algorithms, ToF, blood pool VOI locations and compartment models, in patients with suspected CCS.

Paper III Evaluate the diagnostic accuracy of visual assessment of ICA using qFPP CMR as reference, in patients with suspected CCS.

Paper IV Explore if change in myocardial perfusion assessed with cardiac ^{13}N ammonia PET correlates with change in VO_2 peak assessed with CPET, before and after revascularization.

Paper V Investigate if myocardial perfusion, assessed with qFPP CMR, correlates with variations in serum estradiol levels during the menstrual cycle in pre-menopausal women, as well as non-cyclic estradiol levels in post-menopausal women.

Chapter 3

Materials and Methods

3.1 Study populations

The studies in this thesis were approved by the Swedish National Ethical committee and followed the Declaration of Helsinki. All participants signed informed consent.

Papers I-IV were based on prospectively included patients at Skåne University Hospital, Lund, between 2013 and 2019. The cohort consisted of 100 patients with suspected or established CCS, selected from the elective ICA list. Before and after the ICA, the participants underwent ^{13}N ammonia PET/CT and CMR with adenosine stress and CPET examinations. The participants included from 2016 underwent CMR including qFPP assessment. The angiographer was blinded to the results of the examinations conducted within the study, and decision of revascularization was based on clinically available information. Exclusion criteria were any contraindications for the examinations. All participants were asked to avoid caffeine for 24h before the examinations.

Paper I

In Paper I, 86 patients (median age 69 (range 46-86) years, 24 women) were selected from the main study. Additional exclusion criteria for this study were previous coronary artery bypass graft surgery, dilated or hypertrophic cardiomyopathy, missing ICA data or poor PET image quality. All patients underwent ^{13}N ammonia PET/CT and CMR 2 weeks (range 0-18 weeks) prior to ICA.

Paper II

Twenty-five patients (mean age 70 ± 6 years, nine women) were selected from the cohort of 100 patients. All participants underwent ^{13}N ammonia PET/CT examinations for quantification of myocardial perfusion.

Paper III

Forty-nine patients (median age 70 (range 46-80) years, 15 women) from the main study were eligible for inclusion. Additional exclusion criteria were left bundle branch block, only non-quantitative CMR perfusion images, insufficient CMR image quality and missing ICA data. All patients underwent adenosine stress qFPP CMR 2 weeks (range 0-18 weeks) prior to ICA.

Paper IV

Sixty-two patients (median age 68 (range 46-86) years, 14 females) from the main study were included in this study. Additional exclusion criteria were prior coronary artery bypass graft surgery, hypertrophic or dilated cardiomyopathy, insufficient PET image quality, missing ICA or PET data and failed revascularization attempts during ICA. The patients underwent ^{13}N ammonia PET/CT, CMR and CPET three weeks (range 0-18 weeks) before and 6 months (range 3-20 months) after ICA.

Paper V

Study V was based on prospectively included healthy pre-menopausal (n=12, 26 (range 21-35) years old) and post-menopausal (n=15, 63 (54-72) years old) women that underwent adenosine stress qFPP CMR examinations and blood sample analysis for sex hormone levels at Skåne University Hospital, Lund, 2024-2025. Inclusion criteria for all participants were female sex, age $\geq$ 18 years, ability to give written informed consent and normal ECG at rest. Inclusion criteria specific for pre-menopausal women were age $\leq$ 35 years, regular menstrual cycle with predictable intervals of 25-32 days and body mass index of 18.5-30 kg/m^2. Inclusion criteria specific for post-menopausal women were age $\geq$ 50 years and no vaginal bleeding in the last 12 months. Exclusion criteria for both groups were medications affecting hormone levels or cardiac function, known diseases affecting hormone levels or cardiac health, ongoing breast feeding or pregnancy, blood pressure $>$ 140/90 or $<$ 90 mmHg systolic at rest, caffeine intake $<$ 72h prior to the examination, smoking and any contraindications to undergo adenosine stress CMR.

3.2 Methods

Paper I

^{13}N ammonia PET images were used for assessment of myocardial perfusion at rest and stress, and for calculation of myocardial perfusion reserve (MPR) as a ratio between myocardial perfusion at stress and rest. The myocardial segment of the left ventricle with lowest myocardial perfusion for each main vessel territory (LAD, RCA and LCX) was assessed. The degree of coronary artery stenosis of the culprit lesion (% narrowing) was visually assessed from the coronary angiogram for each main vessel territory. Furthermore, LGE images acquired during the CMR examinations were used to quantify fibrosis of the left ventricle.

Paper II

Global rest, stress and MPR for the left ventricle were assessed from ^{13}N ammonia PET using different time-frame schemes, ToF, reconstruction algorithms, VOI locations and compartment models.

Paper III

Myocardial perfusion at rest and stress was quantified from the qFPP CMR images, and MPR was calculated. Mean perfusion for LAD, RCA and LCX was assessed. Furthermore, the segment with lowest perfusion within each main vessel territory was assessed. Presence of infarction or non-ischemic fibrosis was evaluated from the LGE images. Furthermore, presence of hypertrophic or dilated cardiomyopathy on the CMR images was evaluated. The degree of coronary artery stenosis in % narrowing was assessed visually from the ICA images for LAD, RCA and LCX.

Paper IV

Mean myocardial perfusion at rest, stress and MPR was calculated for LAD, RCA and LCX. Furthermore, global perfusion at stress and MPR for the left ventricle was assessed. VO_2 peak and VO_2 peak % of predicted was calculated from the CPET examination. Presence of fibrosis was assessed from the LGE images.

Paper V

The pre-menopausal women underwent adenosine stress qFPP CMR twice during one menstrual cycle - once in the EFP and once in the MLP. The post-menopausal women underwent the same examination on one occasion. During each examination, blood samples were collected for measurement of sex hormone levels (estradiol, progesterone, testosterone, sex hormone binding globulin, thyroid-stimulating hormone, thyroxin, anti-müllerian hormone, luteinizing hormone and follicle-stimulating hormone). Global myocardial perfusion at rest, stress and MPR was assessed from the qFPP CMR images and compared between EFP and MLP as well as related to serum estradiol levels.

Left ventricle segmentation

The left ventricular myocardium can be divided into 17 segments according to the 17-segment model proposed by the American Heart Association. This 17-segment model is based on the basal, midventricular and apical short axis image slices, positioned 90 degrees towards the long axes of the heart (Figure 3.1)[72, 73]. Segment 17 is the apical segment, and is not included in the three short axis slices acquired with qFPP CMR. Furthermore, due to apical thinning often present in PET images, image quality also poses a challenge for the quantification of myocardial perfusion in segment 17. Therefore, segment 17 was excluded from the analyses in the studies included in this thesis. Furthermore, the segments of the left ventricle can be assigned to the main coronary vessel (LAD, RCA or LCX) supplying the myocardium of the segment. Segments 1, 2, 7, 8, 13, 14, and 17 are supplied by LAD, segments 3, 4, 9, 10, and 15 by RCA and segments 5, 6, 11, 12, and 16 by LCX. However, this is a generalization, since there is anatomical variations of the coronary arteries between individuals[72, 74]. In this thesis, myocardial perfusion was quantified in the qFPP CMR and ^{13}N ammonia PET images to obtain perfusion values in ml/min/g for each segment of the left ventricle.

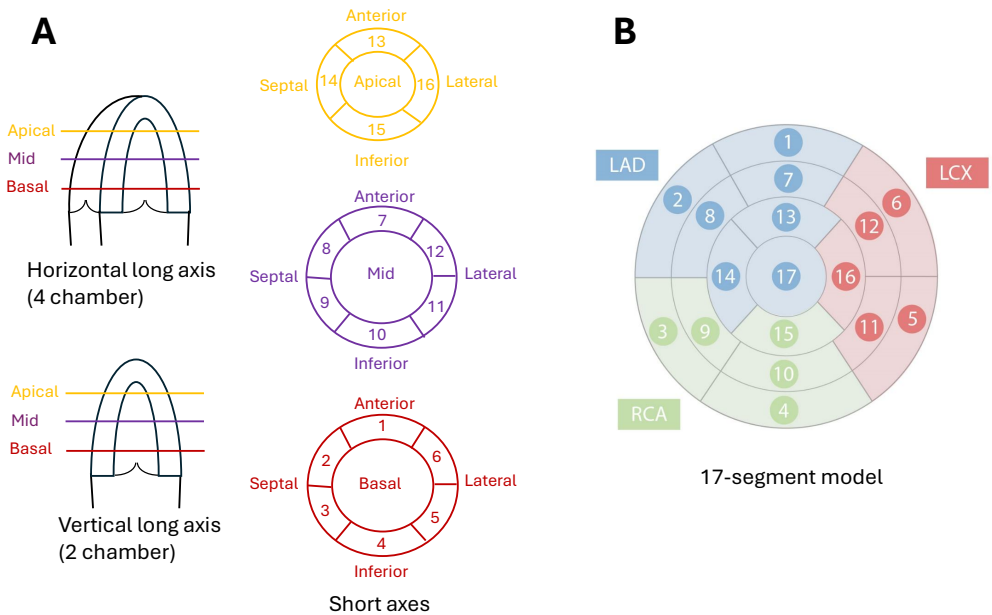

FIGURE 3.1: The horizontal and vertical long axis in relation to the apical, midventricular and basal short axes divided into myocardial segments (A) and the 17-segment model divided according to supplying coronary arteries (B). *LAD = left anterior descending coronary artery, RCA = right coronary artery, LCX = left circumflex coronary artery.*

Cardiac PET acquisition and analysis

The patients underwent ^{13}N ammonia PET examinations with a Discovery 690 PET/CT scanner (GE Healthcare, Waukesha, WI, USA), except in two cases at baseline and one at follow up, when for logistical reasons a Discovery MI PET/CT scanner (GE Healthcare, Waukesha, WI, USA) was used. Image acquisition was done in list mode and total acquisition time was 15 minutes for rest and stress respectively, starting with the rest images followed by a 50-minute break before the stress examination. A scout view of the chest was used for localization of the heart, followed by a low dose CT for the attenuation correction. Image acquisition started during the injection of the radiopharmaceutical with an activity based on the patient's weight, usually 500-550 MBq. For the stress images, adenosine was administered for three minutes at a dose of 140 µg/kg/min [75], increased up to 210 µg/kg/min if absence of adenosine effect was suspected, before image acquisition started. Adenosine infusion continued for four minutes during the acquisition of the dynamic images. Before reconstruction, patient motion between the CT and PET images was checked, and manually adjusted when needed.

For papers I, II and IV, the dynamic images were reconstructed using a time-frame of 5 seconds for the first minute (21 time-frames, framing scheme = 12 × 5 s, 4 × 10 s, 4 × 20 s and 1 × 60 s). Reconstruction was done using OSEM [76] without ToF. The reconstructed images were analyzed in the software Carimas [77]. Endo- and epicardial borders of the left ventricle were delineated automatically and adjusted manually when needed to assess the time-activity curve of the myocardium. A small, basal blood pool VOI was placed in the left ventricle (Figure 3.2) to assess the time-activity curve of the blood pool. The quality of the time-activity curves were checked for each image. Furthermore, the deGrado two-compartment model [36] was used to calculate myocardial perfusion in ml/min/g.

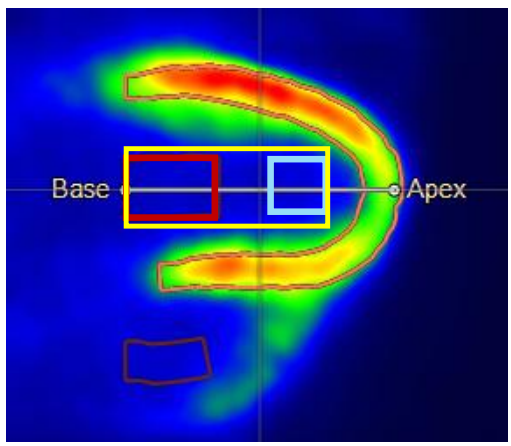

FIGURE 3.2: Long axis PET image with three different blood pool volumes of interest (VOIs) and delineated endo- and epicardium (orange). Red = standard basal VOI. Blue = small apical VOI. Yellow = large VOI from base to apex.

For Paper II, additional image reconstructions and changes of post-processing parameters were performed to assess differences in the quantification of myocardial perfusion. Two other time-frame schemes were used, one of 2 seconds for the first minute (39 time-frames, framing scheme = 30 × 2 s, 4 × 10 s, 4 × 20 s and 1 × 60 s) and one of 10 seconds for the first 12 time-frames (15 time-frames, framing scheme = 12 × 10 s, 2 × 30 s and 1 × 60 s). Reconstruction was performed using the block-sequential regularized expectation maximization (BSREM) algorithm, known to reduce the background noise of the image[78,79]. Furthermore, reconstruction using ToF was conducted, as was image analysis with a small apical VOI and a large VOI from apex to base (Figure 3.2). Additionally two different compartment models - Hutchins[38] (three-compartment model) and Krivokapich[37] (two-compartment model) - were used for perfusion quantification. Table 3.1 summarizes the different reconstructions and analyses.

TABLE 3.1: Different reconstruction and image analysis parameters for Paper II to assess myocardial perfusion.

	Time-frame	Recon. algorithm	ToF	VOI placement	Comp. model
$MBF_{standard}$	5 s	OSEM	no	basal	deGrado
MBF_{2s}	2 s	OSEM	no	basal	deGrado
MBF_{10s}	10 s	OSEM	no	basal	deGrado
MBF_{BSREM}	5 s	BSREM	no	basal	deGrado
MBF_{ToF}	5 s	OSEM	yes	basal	deGrado
$MBF_{ApicalVOI}$	5 s	OSEM	no	apical	deGrado
$MBF_{LargeVOI}$	5 s	OSEM	no	large	deGrado
$MBF_{Hutchins}$	5 s	OSEM	no	basal	Hutchins
$MBF_{Krivokapich}$	5 s	OSEM	no	basal	Krivokapich

MBF = myocardial blood flow, BSREM = block-sequential regularized expectation maximization, ToF = time-of-flight, VOI = volume of interest, OSEM = ordered subset expectation maximization

CMR acquisition and analysis

The patients in papers I, III and IV underwent CMR examinations using a 1.5 T Philips Achieva (Best, the Netherlands) or MAGNETOM Aera (Siemens Healthineers, Forchheim, Germany). Two different scanner were used due to an exchange of scanners after the study started. The healthy women of Paper V underwent CMR using a 1.5 T MAGNETOM Sola (Siemens Healthineers, Forchheim, Germany), except for one post-menopausal woman who was examined with the MAGNETOM Aera.

Scout imaging was done for the localization of the heart, followed by the planning of the 2-, 3- and 4-chamber views and the short axis. The stress perfusion images were acquired first. Adenosine infusion began at 140 µg/kg/min, and was increased up to 210 µg/kg/min if absence of adenosine effect was suspected[43]. For Paper V specifically, the adenosine dose was kept constant at 140 µg/kg/min. Image acquisition began during the first pass of a 0.05 mmol/kg bolus of a gadolinium-based contrast agent. For papers I, III, and IV, the agent used was Dotarem (Guerbet, Roissy, France and Gothia Medical, Billdal, Sweden), while Clariscan (gadoterate meglumine, GE Healthcare, Danderyd, Sweden) was used for Paper V. Adenosine infusion continued during the acquisition. The qFPP maps in the basal, midventricular and apical short-axis view as well as 2-, 3- and 4-chamber views were acquired using the single-bolus, dual-sequence approach[48] and reconstructed using Gadgetron[51]. Approximately 10 minutes after the stress acquisition, the perfusion images at rest were acquired.

The short axis cine images covering the left ventricle were acquired after the perfusion sequences. For Paper V, multi-parametric SAturation-recovery single-SHot Acquisition (mSASHA) short-axis T1 and T2 maps were acquired pre and post contrast agent administration[80]. LGE images in the short axis and long stacks were acquired approximately 10 minutes after the last top-off dose of contrast agent was injected[81].

All CMR image analyses were done using the software Segment (Medviso, Sweden, http://segment.heiberg.se)[82]. The short-axis qFPP maps were manually delineated at the endo- and epicardial borders. Right ventricular insertion points were placed in the midventricular slice to indicate the orientation of the left ventricle (Figure 3.3). Myocardial perfusion at rest and stress was quantified according to the 17-segment model[72]. Furthermore, MPR was calculated as the ratio of myocardial perfusion at stress and rest. In Paper III, myocardial perfusion at stress < 2.0 ml/min/g and MPR < 2.4 was considered significantly reduced[83].

Left ventricular mass and ejection fraction were assessed by manual delineation of endo- and epicardial borders at end-systole and end-diastole of the left ventricle short axis cine images covering the left ventricle, according to guidelines[84].

Presence and location of infarction and/or non-ischemic fibrosis was assessed visually on the LGE images and assigned a main vessel territory. In Paper I, infarction and non-ischemic fibrosis were quantified using the EWA algorithm[85] and expressed as % of left ventricular mass.

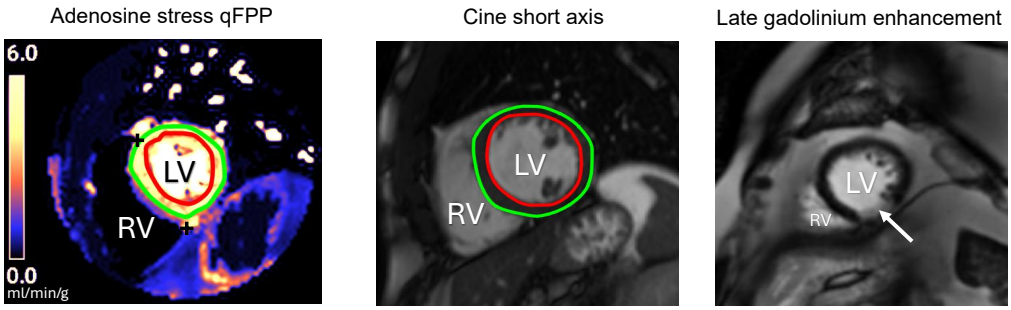

FIGURE 3.3: Delineated endocardial (green) and epicardial (red) borders of an adenosine stress qFPP map (left) and a cine short axis image (middle). The right ventricular insertion points are indicated by the black crosses in the qFPP map. A late gadolinium enhancement image (right) is shown with a white arrow indicating a myocardial infarction. *LV = left ventricle, RV = right ventricle.*

The mSASHA T1 and T2 maps were manually delineated at the endo- and epicardial borders in the basal, midventricular and apical short axis images. Right ventricle insertion points and a left ventricular lumen blood pool region of interest were defined in the midventricular short axis slice. The ECV was calculated as previously described [44]:

$$\mathrm{ECV} = (1 - \mathrm{Hct}) \cdot \left(\frac{\frac{1}{T1_{\mathrm{postmyo}}} - \frac{1}{T1_{\mathrm{premyo}}}}{\frac{1}{T1_{\mathrm{postblood}}} - \frac{1}{T1_{\mathrm{preblood}}}} \right)$$

ECV = extracellular volume, Hct = hematocrit, $T1_{premyo}$ = T1 time pre contrast in the myocardium, $T1_{postmyo}$= T1 time post contrast in the myocardium, $T1_{preblood}$ = T1 time pre contrast of the blood pool, $T1_{postblood}$ = T1 time post contrast of the blood pool.

ICA analysis

ICA was performed according to clinical routine at Skåne University Hospital, Lund. The coronary angiograms were analyzed visually by an experienced interventional cardiologist. The culprit lesion for each main coronary vessel (LAD, RCA and LCX) was defined as estimated luminal diameter narrowing and reported in %. The interventional cardiologist assessing the angiograms was blinded to the results of the examinations performed within the study. In Paper III, coronary artery stenoses $\geq 70\%$ were considered significant[9].

CPET analysis

The CPET examinations were performed at Skåne University Hospital, Lund, using a cycle ergometer. The starting workload and the ramp gradient were based on the patient's sex, age and baseline fitness level, and were repeated for the follow up examination. VO_2 peak was determined at peak workload in ml/min and adjusted for patient weight (ml/min/kg). Furthermore, VO_2 peak % of predicted value was calculated[64].

Evaluation of the menstrual cycle

In Paper V, the qFPP CMR examinations were scheduled according to the participant's menstrual cycle (Figure 3.4). The first examination was conducted in the EFP during day 2-5 of the menstrual cycle, with low levels of estrogen and progesterone. The day of expected ovulation during the ongoing menstrual cycle was estimated as expected first day of the next cycle minus 14 days[22]. Participant were provided with urine test kits to check luteinizing hormone levels, which they used daily from five days before expected ovulation. A positive test result indicated that ovulation will occur within the next 24-48 hours. The second examination was planned 6-8 days after a positive luteinizing hormone test result - in the MLP phase when there are expected to be high levels of estrogen and progesterone. On the same day as each examination, pregnancy tests measuring human chorionic gonadotropin were performed to exclude pregnancy.

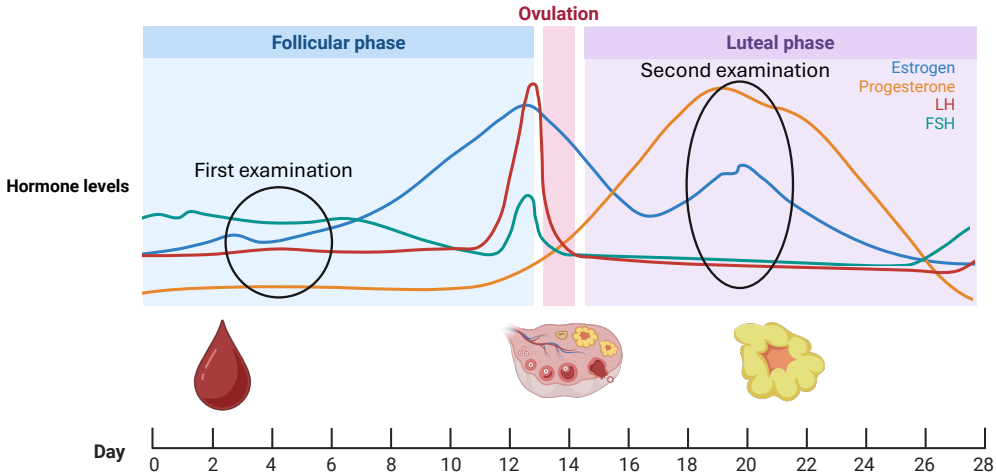

FIGURE 3.4: A schematic illustration of the hormone levels during the menstrual cycle. The first qFPP CMR examination was done in the early follicular phase, when the hormone levels are low. The second examination was done after ovulation, in the mid-luteal phase, when estrogen and progesterone levels are high. *LH = luteinizing hormone, FSH = follicle-stimulating hormone. Created in BioRender. Szekely, A. (2025) https://BioRender.com/9p643xp*

Statistics and figures

Statistical analyses were done using GraphPad Prism (GraphPad Software, Boston, Massachusetts, USA) and SPSS (Armonk, NY: IBM Corp). Continuous data was presented as mean ± standard deviation or median (range) when the distribution was skewed. In Paper V, D'Agostino and Pearson tests were used to assess normal distribution. Paired t-tests were used to compare paired continuous parametric variables, and Wilcoxon tests were used for paired continuous non-parametric variables. MannWhitney's non-parametric test was used to compare continuous non-parametric variables between groups. Pearson's correlation coefficient was used to correlate parametric continuous variables, and Spearman's rank correlation coefficient was used to correlate non-parametric continuous variables. Interobserver variability was analyzed using Bland-Altman (Paper I) or intra-class correlation coefficients. In Paper I, linear mixed model analyses were performed to assess the independent association between different variables and myocardial perfusion, taking multiple measurements for each patient into consideration. For Paper II, Bland-Altman analyses[86] were used to assess the agreement between the perfusion assessed with different reconstruction and post-processing parameters. For Paper III, sensitivity, specificity and accuracy for ICA using qFPP CMR as reference was calculated. Furthermore, area under the receiver-operator characteristic curve was presented with 95% confidence interval. A P value < 0.05 was considered to indicate statistical significance in all papers.

Graphs were produced using GraphPad (GraphPad Software, Boston, Massachusetts, USA). Images were produced in Inkscape (The Inkscape Project, https://inkscape.org) or Biorender (https://www.biorender.com/).

Chapter 4

Results

4.1 Paper I

Paper I investigated to what extent sex, age, hypertension, diabetes and smoking affect myocardial perfusion assessed with ^{13}N ammonia PET independent of degree of coronary artery stenosis in patients with suspected CCS.

Sex differences

The results showed that men have significantly lower myocardial perfusion at stress ($P < 0.001$) and rest (P=0.002) than women, but there was no difference in MPR (P=0.081). The difference in myocardial perfusion at stress between sexes was only found in the vessel territories with ≤ 50 % coronary artery stenosis ($P < 0.001$), while there was no difference between sexes in vessel territories with $> 50\%$ stenosis (P=0.16) (Figure 4.1).

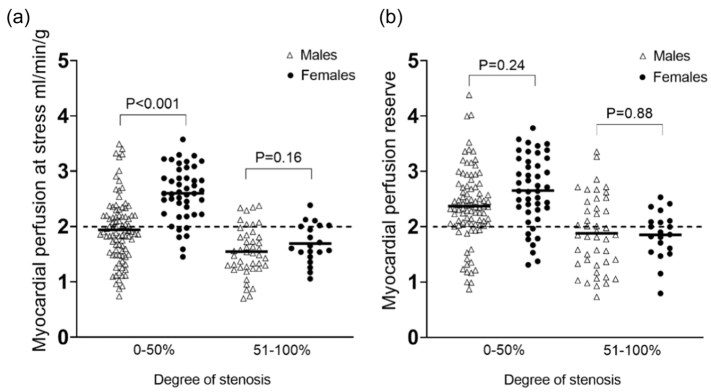

FIGURE 4.1: Myocardial perfusion at stress (a) and myocardial perfusion reserve (b) in vessel territories with 0-50% and 51-100% coronary artery stenoses, divided by sex. *Solid lines indicate mean perfusion in each group. Dashed lines indicate a cut off for myocardial perfusion at 2.0 ml/min/g.*

Age, hypertension, diabetes and smoking

Older age was associated with lower myocardial perfusion at stress (P=0.025) and MPR (P=0.040). Patients with hypertension had lower MPR than normotensive patients (P=0.033), and patients with diabetes had lower myocardial perfusion at stress than non-diabetic patients (P=0.023). However, there was no difference in myocardial perfusion between current or previous smokers and non-smokers (Figure 4.2).

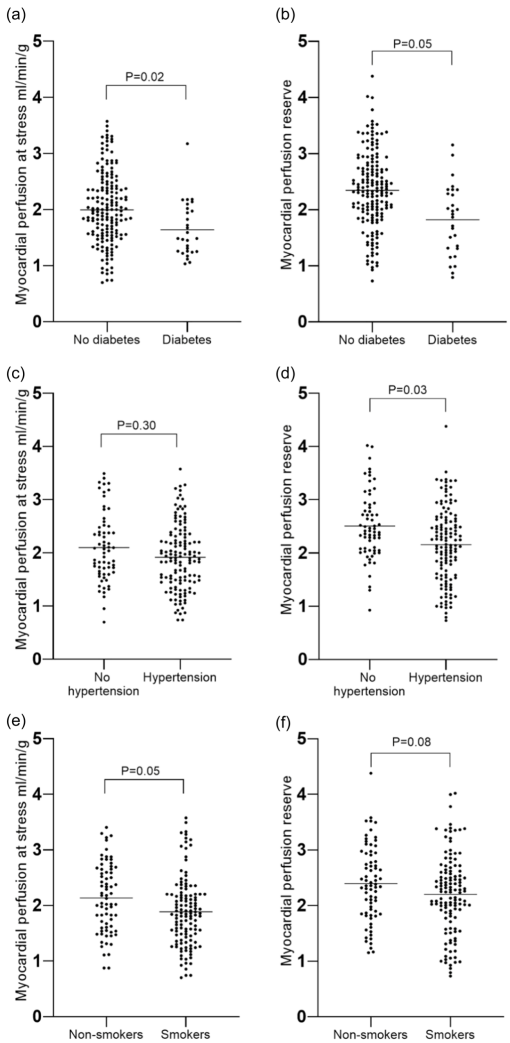

FIGURE 4.2: Myocardial perfusion at stress (left column) and myocardial perfusion reserve (right column) divided between diabetic and non-diabetic patients (a and b), hypertensive and normotensive patients (c and d) and smokers and non-smokers (e and f).

4.2 Paper II

In Paper II, different reconstruction and post-processing methods for global myocardial perfusion assessed with ^{13}N ammonia PET were compared. The standard assessment of myocardial perfusion used the time-frame scheme of 5 seconds, reconstruction model OSEM, without ToF, with a basal blood pool VOI and the deGrado compartment model. All adjustments of reconstruction and post-processing methods (Table 3.1) were compared to this standard assessment.

Myocardial perfusion at stress and rest

Global myocardial perfusion in ml/min/g assessed using different time-frame schemes (5s versus 2s or 10s) and reconstruction algorithms (OSEM versus BSREM) showed good agreement (standard versus 2s: 0.02 ± 0.06; 10s: 0.01 ± 0.07; BSREM: 0.01 ± 0.07). However, global myocardial perfusion assessed with and without ToF, with different blood pool VOI placements (basal versus apical or large) and with different compartment models (deGrado versus Hutchins or Krivokapich) showed a lower level of agreement (standard verus ToF: 0.07 ± 0.10; apical VOI: 0.27 ± 0.25; large VOI: 0.11 ± 0.10; Hutchins: 0.08 ± 0.10; Krivokapich: 0.47 ± 0.50) (Figure 4.3). Similar results were seen both when stress and rest were analyzed together and when analyzed separately.

Myocardial perfusion reserve

Good agreement was shown between global MPR assessed with different time-frame schemes (5s versus 2s or 10s), with and without ToF, and between the deGrado and Hutchins compartment models (standard versus 2s: 0.01 ± 0.12; 10s: 0 ± 0.14; ToF: 0.01 ± 0.20; Hutchins: 0 ± 0.22). A lower level of agreement was seen when MPR was assessed using different reconstruction algorithms (OSEM versus BSREM), different blood pool VOI placements (basal versus apical or large), and between the deGrado Krivokapich compartment models (standard versus BSREM: 0.06 ± 0.14; apical VOI: 0.20 ± 0.27; large VOI: 0.10 ± 0.10; Krivokapich: 0.45 ± 0.38) (Figure 4.4).

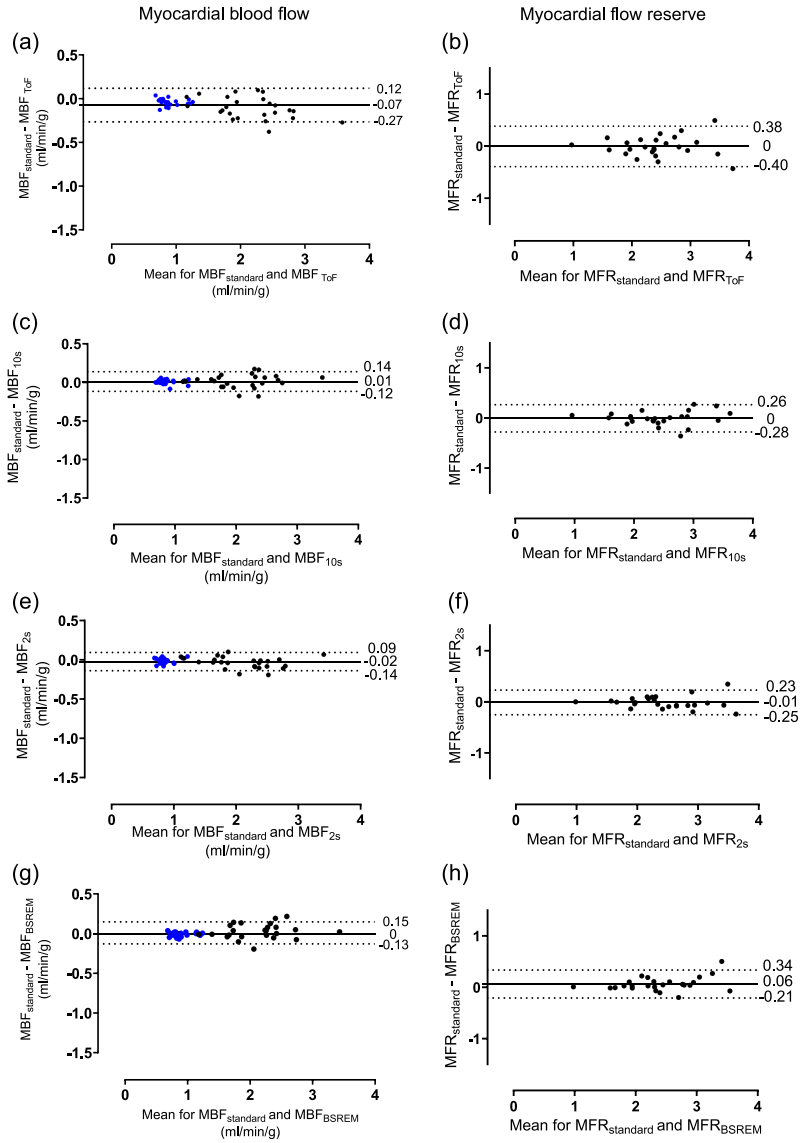

FIGURE 4.3: Bland-Altman plots for the agreement between global myocardial perfusion (left column) and myocardial perfusion reserve (right column) assessed with the standard parameters and with ToF (a and b), time-frame scheme of 10s (c and d) or 2s (e and f) and reconstruction with BSREM (g and h). The solid lines indicate the mean difference, the dashed lines the limits of agreement (+2SD and -2SD). The blue dots represent perfusion at rest and the black dots perfusion at stress. *MBF = myocardial blood flow (synonym to myocardial perfusion), MFR = myocardial flow reserve (synonym to myocardial perfusion reserve), ToF = time-of-flight, BSREM = block-sequential regularized expectation maximization.*

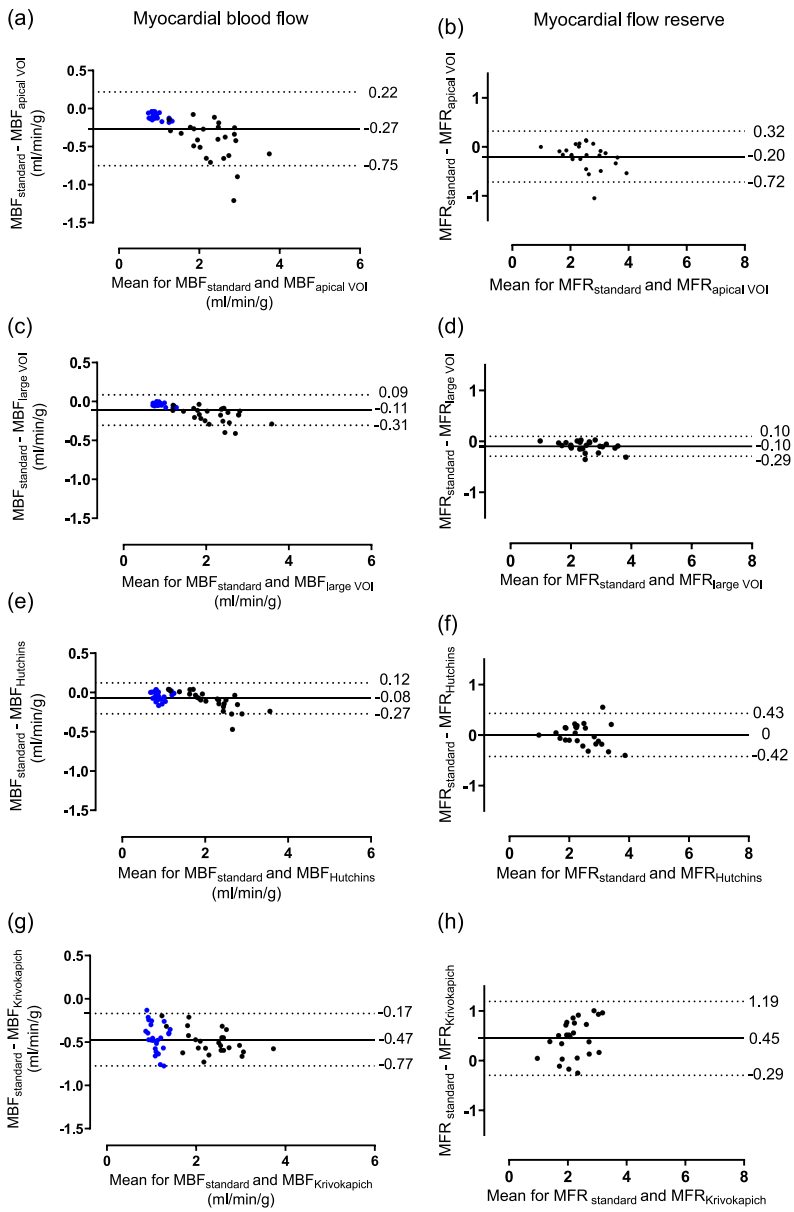

FIGURE 4.4: Bland-Altman plots for the agreement between global myocardial perfusion (left column) and myocardial perfusion reserve (right column) assessed with the standard parameters and with apical VOIs (a and b), large VOIs (c and d), Hutchins compartment model (e and f) and Krivokapich compartment model (g and h). The solid lines indicate the mean difference, the dashed lines the limits of agreement (+2SD and -2SD). The blue dots represent perfusion at rest and the black dots perfusion at stress. *MBF = myocardial blood flow (synonym to myocardial perfusion), MFR = myocardial flow reserve (synonym to myocardial perfusion reserve), VOI = volume of interest.*

4.3 Paper III

This study investigated the diagnostic accuracy of ICA to detect reduced myocardial perfusion acquired with qFPP CMR. Myocardial perfusion for each main vessel territory (LAD, RCA and LCX) was defined in two ways: 1) As the myocardial segment of each main vessel territory with lowest myocardial perfusion (myocardial perfusion$_{\text{min}}$ and MPR$_{\text{min}}$) 2) As the mean perfusion of all segments within each main vessel territory (myocardial perfusion$_{\text{mean}}$ and MPR$_{\text{mean}}$).

Sensitivity, specificity and accuracy

Table 4.1 shows the sensitivity, specificity and accuracy for visual assessment of ICA (cut-off 70 % of coronary artery stenosis) for detecting reduced myocardial perfusion at stress ($<$ 2.0 ml/min/g) or MPR ($<$ 2.4). The lowest sensitivity and specificity for ICA was seen when MPR$_{\text{mean}}$ was used as reference (sensitivity 32%, specificity 70%). Figure 4.5 shows examples of when qFPP CMR and ICA match and when they mismatch.

TABLE 4.1: Sensitivity, specificity and accuracy for visual assessment of ICA to detect reduced myocardial perfusion.

	Sensitivity	Specificity	Accuracy
Myocardial perfusion$_{\text{min}}$ at stress	36%	76%	0.55
Myocardial perfusion$_{\text{mean}}$ at stress	41%	73%	0.64
Myocardial perfusion$_{\text{min}}$ reserve	34%	75%	0.48
Myocardial perfusion$_{\text{mean}}$ reserve	32%	70%	0.55

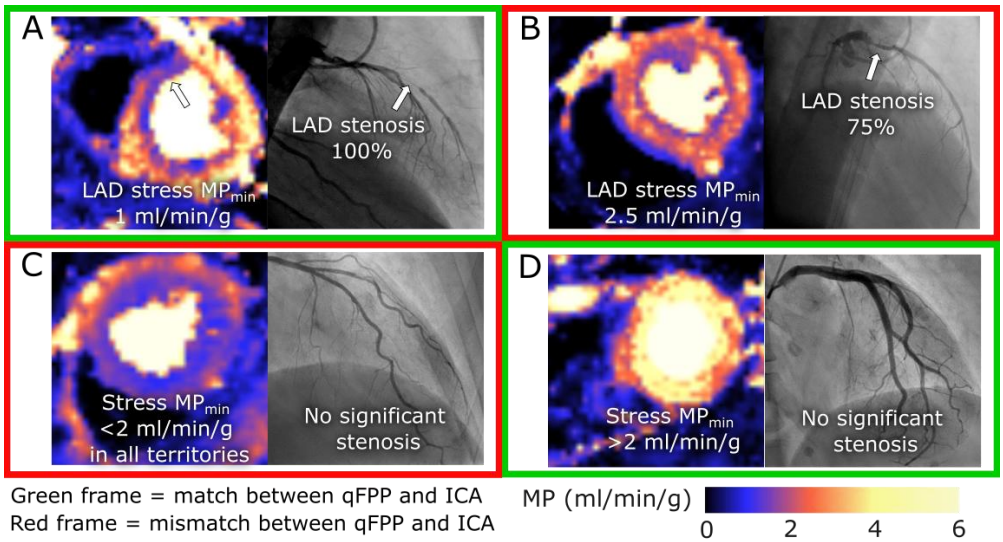

FIGURE 4.5: Examples of when myocardial perfusion and invasive coronary angiography match (green frames) and when they mismatch (red frames). *LAD= left anterior descending coronary artery, MP = myocardial perfusion.*

Correlation

Degree of coronary artery stenosis correlated significantly with myocardial perfusion$_{min}$ at stress (R = -0.27, p = 0.006). However, degree of coronary artery stenosis did not correlate with myocardial perfusion$_{mean}$ at stress, MPR$_{min}$ or MPR$_{mean}$. Figure 4.6 shows the relationship between myocardial perfusion and degree of coronary artery stenosis.

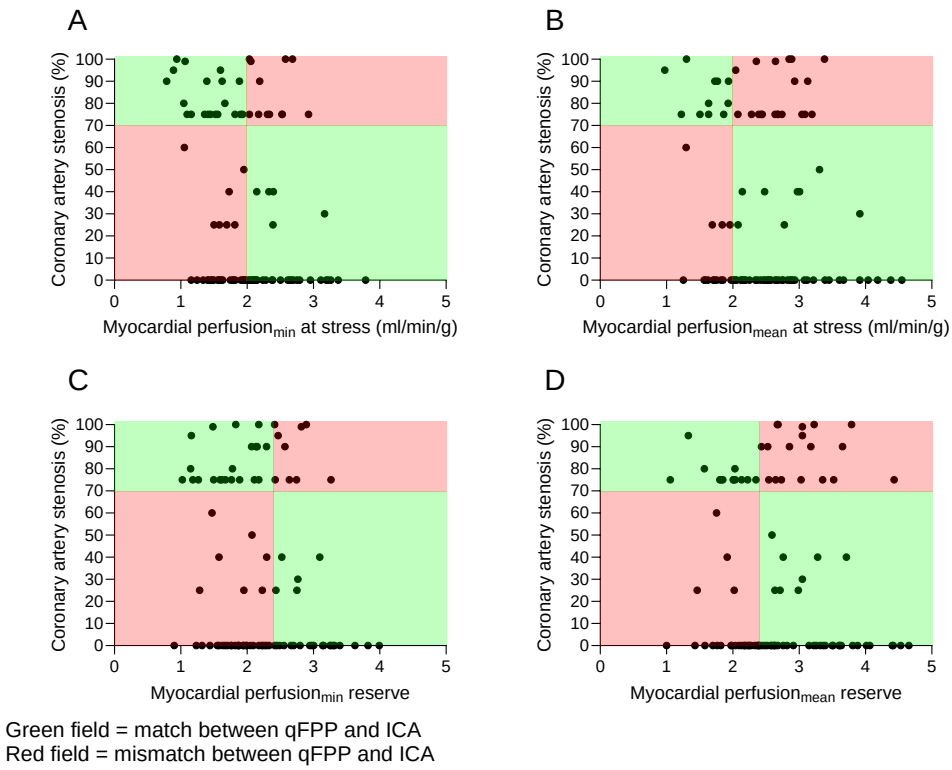

FIGURE 4.6: The relationship between degree of coronary artery stenosis visually assessed from the coronary angiography and myocardial perfusion$_{min}$ at stress (A), myocardial perfusion$_{mean}$ at stress (B), myocardial perfusion$_{min}$ reserve (C) and myocardial perfusion$_{mean}$ reserve (D). Red fields indicate a mismatch between myocardial perfusion and coronary angiography findings and green fields indicate a match.

4.4 Paper IV

In this study, the correlation between change in myocardial perfusion and VO_2 peak before and after revascularization was explored.

Change in myocardial perfusion

In total, 47 vessel territories in 35 patients were revascularized by PCI or coronary artery bypass graft surgery between baseline and follow up PET examinations. Mean myocardial perfusion at stress in revascularized vessel territories increased significantly after revascularization, both when perfusion was < 2.0 ml/min/g (P=0.006) and when perfusion was ≥ 2.0 ml/min/g (P=0.008) in the vessel territory at the baseline PET examination. Mean MPR in revascularized vessel territories only increased significantly after revascularization when baseline MPR was < 2.4 ($P < 0.001$), and not when baseline MPR was ≥ 2.4 (P=0.41). Global myocardial perfusion at stress and global MPR only increased significantly after revascularization when baseline perfusion was reduced (stress P=0.02, MPR P=0.001) (Figure 4.7).

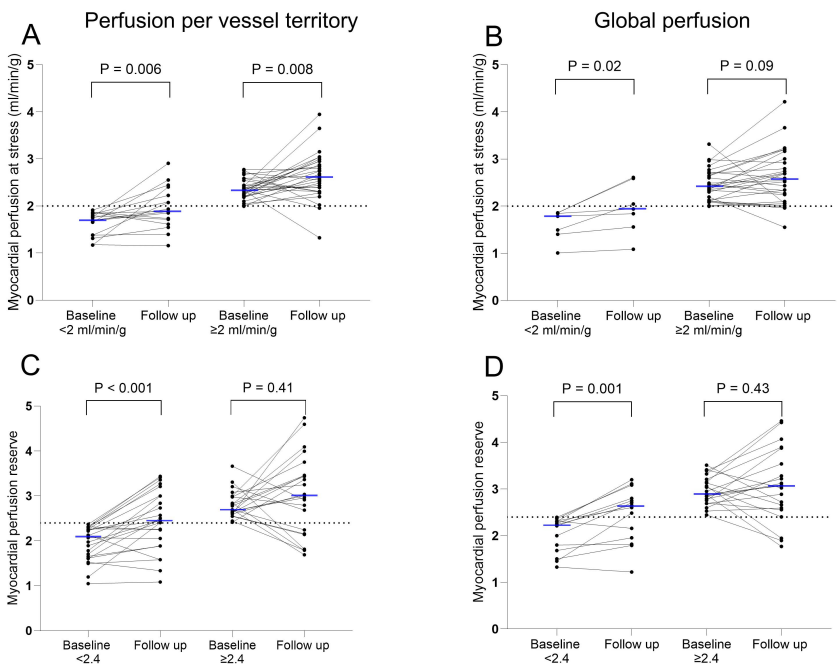

FIGURE 4.7: Myocardial perfusion at stress (A and B) and myocardial perfusion reserve (C and D). The left column shows perfusion per vessel territory from baseline to follow-up in revascularized vessel territories. The right column shows global perfusion in revascularized patients. The cohort was divided according to baseline perfusion - indicated by the dotted lines. Blue solid lines indicate median perfusion in each group.

VO_2 peak and VO_2 peak % of predicted

No change in VO_2 peak or VO_2 peak % of predicted value was seen from baseline to follow-up in either the revascularized or non-revascularized groups. Furthermore, change in VO_2 peak or VO_2 peak % of predicted value from baseline to follow-up did not correlate with change in global myocardial perfusion at stress or MPR in either revascularized patients (Figure 4.8) or non-revascularized patients. No significant change in VO_2 peak and VO_2 peak % of predicted value was seen in patients undergoing revascularization of vessel territories with significantly reduced baseline myocardial perfusion at stress (< 2.0 ml/min/g, P=0.63 and P=0.94) or MPR (< 2.4, $P > 0.99$ and P=0.96).

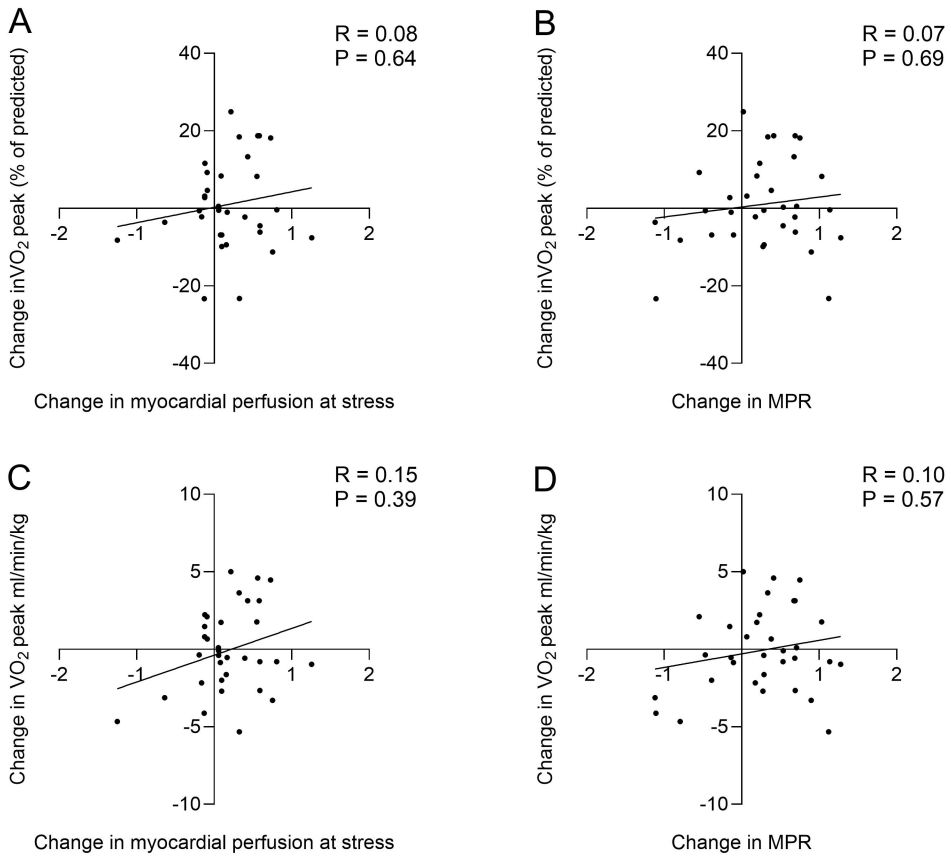

FIGURE 4.8: The upper row shows correlations between change in VO_2 peak % of predicted value and myocardial perfusion at stress (A), and myocardial perfusion reserve (B), in revascularized patients. The lower row shows correlations between change in VO_2 peak and myocardial perfusion at stress (C), and myocardial perfusion reserve (D), in the same patients. *MPR = myocardial perfusion reserve.*

4.5 Paper V

Paper V investigated the relationship between estradiol levels and myocardial perfusion in healthy pre- and post-menopausal women.

Myocardial perfusion during the menstrual cycle

Global myocardial perfusion at rest increased from EFP to MLP in the pre-menopausal women (P=0.03). There was no significant change in global myocardial perfusion at stress from EFP to MLP (P=0.54). However, global MPR decreased significantly from EFP to MLP (P=0.03) (Figure 4.9). Additionally, native T1, T2 and ECV did not change from EFP to MLP.

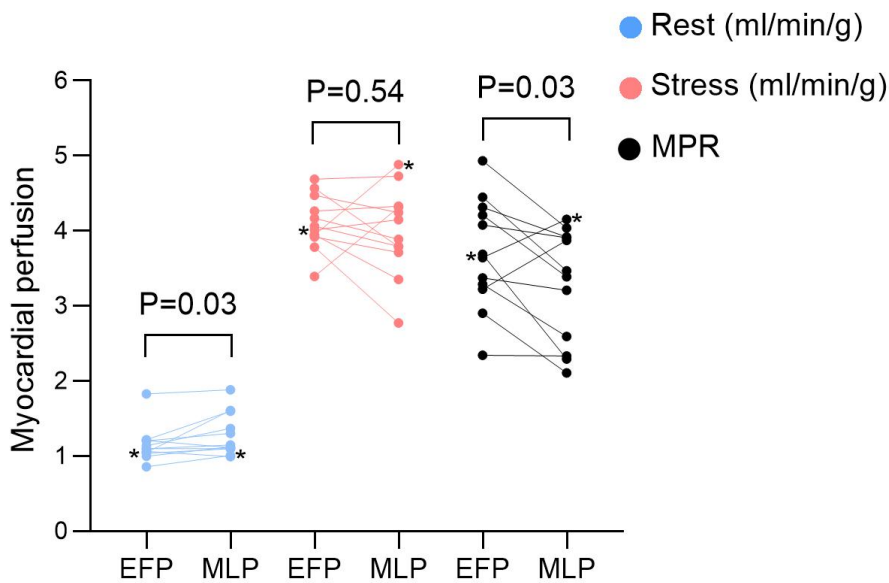

FIGURE 4.9: Global myocardial perfusion at rest (blue), stress (red) and MPR (black) in EFP versus MLP. The asterisks mark a woman with an anovulatory cycle. *EFP = early follicular phase; MLP = mid-luteal phase, MPR = myocardial perfusion reserve.*

Myocardial perfusion in relation to estradiol levels

Global myocardial perfusion at stress and global MPR was lower with higher serum estradiol levels in pre-menopausal women (R=-0,45, P=0.03 and R=-0.47, P=0.02). Furthermore, global myocardial perfusion at stress was lower with higher serum estradiol levels in post-menopausal women (R=-0.53, P=0.045). However, there was no correlation between global MPR and estradiol levels in the post-menopausal women (R=-0.42, P=0,12). Global myocardial perfusion at rest did not correlate with serum estradiol levels in either pre- or post-menopausal women (R=0.31, P=0.14 and R=-0.19, P=0.50) (Figure 4.10).

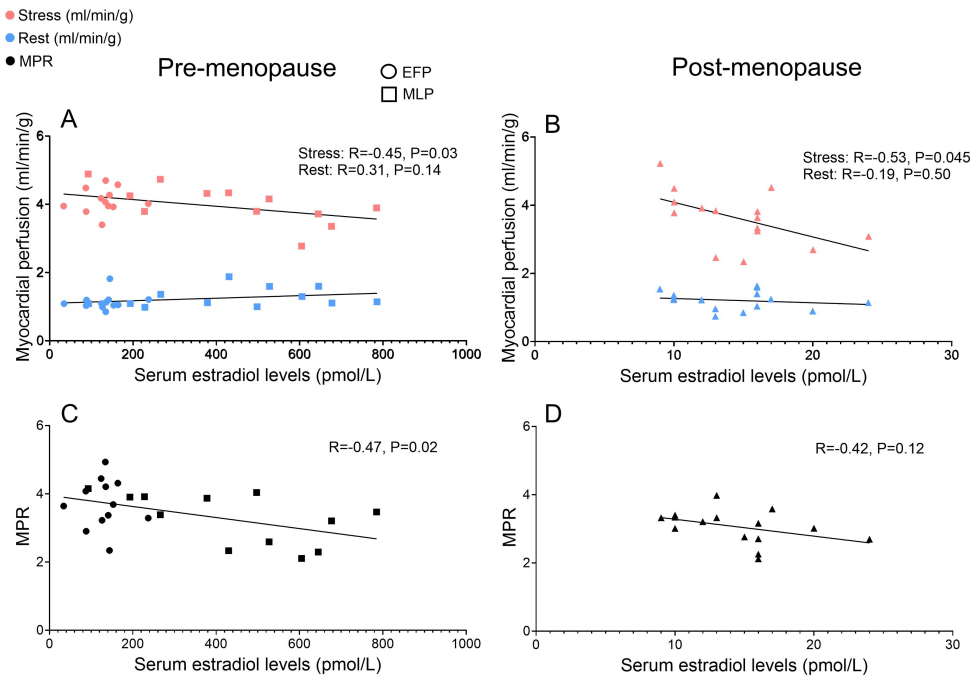

FIGURE 4.10: Correlations between serum estradiol levels and myocardial perfusion at stress, rest and MPR in pre-menopausal women (A and C) and post-menopausal women (B and D). The pre-menopausal data points are divided according to time of acquisition - during EFP (circles) or during MLP (squares). *EFP = early follicular phase; MLP = mid-luteal phase, MPR = myocardial perfusion reserve*

Chapter 5

Discussion

The main findings of this thesis showed that myocardial perfusion can be affected by several patient-specific and methodological factors and is not coherent with visual findings on ICA. Furthermore, improvement in perfusion after revascularization is not correlated to change in VO_2 peak.

Paper I and II highlighted factors that need to be considered when implementing normal values for myocardial perfusion, to be able to evaluate the presence of ischemia using quantitative myocardial perfusion modalities. Paper I showed that independently of the presence of a coronary artery stenosis, myocardial perfusion is affected by sex, age, hypertension, diabetes and smoking. To the best of our knowledge, Paper II is the first study to evaluate to what extent the different reconstruction and post-processing parameters investigated affect myocardial perfusion quantification using ^{13}N ammonia PET. Hence, paper II showed that the determination of normal values for myocardial perfusion needs to consider the method used for quantification. Normal values of myocardial perfusion at stress and MPR for both qFPP CMR[83, 15, 47, 87] and cardiac PET[88, 89, 90] have been proposed by previous studies. Several of these studies have taken sex and age differences into consideration when proposing normal values, which might improve the detection of CCS. The potential of improving outcome for patients with suspected CCS if implementing patient-specific normal values for myocardial perfusion evaluation remains to be investigated.

The results of Paper V indicated that myocardial perfusion at stress and MPR might decrease with increasing estradiol levels. To the best of our knowledge, this is the first study investigating how myocardial perfusion assessed with qFPP CMR changes during the menstrual cycle in pre-menopausal women. The results of this study might contribute to our understanding of the physiological determinants behind the sex differences in cardiac function. Estrogen has shown to decrease microvascular resistance[91]. Therefore, it would be expected that at higher estrogen levels, the vasodilation induced by adenosine would increase, and thereby increasing myocardial perfusion at stress. However, this contradicts the results of Paper V. A potential explanation to the results of Paper V could partly be that at lower estrogen levels, the oxygen demand of the myocardium increases, as shown in animal experimental models[92, 93]. Increased oxygen demand of the myocardium could potentially increase myocardial perfusion at stress in women without CCS. Furthermore, the increased oxygen demand when estrogen levels

are low may induce more ischemia at stress in patients with CCS, than when estrogen levels are high. This is supported by previous findings showing that pre-menopausal women with angina often experience worse symptoms during menstruation [94], and that myocardial ischemia is more easily induced during exercise testing in the EFP than in the the MLP [95]. Paper V did not include any women with cardiac diseases. The WISE study showed that patients with coronary artery disease have lower estradiol levels than healthy controls [96] and Knuuti et al. showed that MPR increases with hormone therapy in women with angina [18]. Higher estrogen levels may be cardioprotective both due to estrogen's effect on the alterations of the cardiac vasculature, increasing perfusion at stress in women with CCS, and by decreasing the oxygen demand of the myocardium, decreasing perfusion at stress in healthy women. However, the explanations to the potential effect of estrogen on myocardial perfusion needs to be further investigated.

Microvascular dysfunction has gained attention over the last years. The difference in myocardial perfusion due to hypertension, diabetes and smoking presented in Paper I might be explained by the increased risk of microvascular dysfunction in these patients, lowering the myocardial perfusion without the presence of obstructive coronary artery disease [97, 98, 99]. The mismatch between qFPP CMR and visual assessment of ICA shown in Paper III might be partly explained by the presence of microvascular dysfunction. More than half of women undergoing elective ICA due to suspected CCS present with non-obstructive coronary artery disease, compared to one third of men [100]. Patients with non-obstructive coronary artery disease on ICA have a high prevalence of microvascular dysfunction [101] and women presenting with non-obstructive coronary artery disease on angiograms have worse outcomes than men [102]. The CorMica trial recently showed that medical therapy improves outcomes for patients with microvascular dysfunction [103]. While imaging modalities depicting the relative perfusion distribution of the myocardium might overlook the presence of global microvascular dysfunction, qFPP CMR and cardiac PET enable the assessment of globally reduced perfusion caused by microvascular dysfunction. Kotecha et al. have proposed different cut-off values for myocardial perfusion assessed using CMR, to differentiate between obstructive coronary artery disease, defined by fractional flow reserve, and microvascular dysfunction, defined by index of microcirculatory resistance. Hence, using non-invasive quantitative perfusion imaging can improve the detection of microvascular dysfunction [47].

The results of paper III and IV highlight the need of functional evaluation of coronary artery stenoses prior to revascularization, to avoid unnecessary interventions. The relationship between degree of coronary artery stenosis assessed visually from ICA and the functional significance on downstream perfusion has previously been shown to be weak [7]. Paper III confirmed this by using qFPP CMR as reference method. Paper IV, and previously Akil et al on the same patient population [104], showed that revascularization mainly improves myocardial perfusion when baseline perfusion is significantly reduced. The benefit of revascularization compared to medical therapy alone has been questioned by the ISCHEMIA trial [105] and the COURAGE trial [106]. However, the evaluation of ischemia in these trials was based on a variety of different examinations, including exercise stress testing, which is not recommended for ischemia evaluation in the current guidelines [4]. Quantitative assessment of myocardial perfusion has shown good ability to detect obstructive coronary artery disease and microvascular dysfunction [47, 24, 88, 107, 108, 109] and has been shown to be a strong predictor of adverse car-

diovascular outcomes[83, 110]. The CE-MARC II trial demonstrated that a strategy of using CMR or single photon emission computed tomography to guide revascularization led to fewer unnecessary angiographies than when following the UK National Institute for Health and Care Excellence guidelines[111, 112]. Furthermore, a recent study showed that first pass perfusion CMR can detect extensive myocardial ischemia in need of revascularization, improving outcome for patients with multivessel disease[113]. Hence, non-invasive assessment of ischemia prior to ICA is currently recommended by the guidelines for management of patients with CCS, to avoid unnecessary invasive procedures[4].

In Paper IV, we showed that change in myocardial perfusion after revascularization does not correlate to change in VO_2 peak. Hence, revascularization itself is not expected to improve VO_2 peak in patients with CCS. The ORBITA trial and the ISCHEMIA trial showed that PCI leads to less angina in patients with CCS[114, 115]. However, the ORBITA trial also showed that undergoing PCI does not increase exercise capacity[116], which is in line with the results of Paper IV. In Paper IV, the choice of revascularization was not based on the results from the stress perfusion examinations. However, a subgroup analysis of patients undergoing revascularization of vessel territories with reduced myocardial perfusion, defined as <2 ml/min/g, did not show any correlation with change in VO_2 peak. These results indicate that despite revascularization of ischemic vessel territories, exercise capacity does not improve. A potential explanation is that the relationship between myocardial perfusion and exercise capacity is more complex, and is to a large extent influenced by other factors - for example exercise habits, medications and comorbidities as well as peripheral factors affecting gas exchange.

To conclude, quantitative myocardial perfusion imaging has a significant role in the clinical workflow for evaluating patients with suspected stress induced ischemia, and this thesis aimed to increase the understanding of the determinants of myocardial perfusion, to improve the diagnostics of patients with CCS.

Limitations

The results in this thesis should be interpreted in the light of some limitations.

The 17-segment model[72] was used to divide the left ventricle into vessel territories in papers I, III and IV. However, as mentioned in the methods section, individual anatomical variation is known to exist[74], and segments might be perfused by a main coronary artery other than the one presented in the model. This was partly corrected for in Paper I by visual assessment of the stress perfusion images in patients with coronary artery stenoses present on the ICA. If there was an ischemic area in adjacent segments of other vessel territories, those segments were considered to be supplied by the stenotic vessel.

All CMR and PET examinations in the current thesis used adenosine as stressor. As mentioned in the introduction section, inadequate adenosine effect might lead to false low myocardial perfusion at stress. In Paper III, absence of adenosine effect could explain some of the cases where myocardial perfusion was decreased despite no coronary artery stenosis. However, only one patient in this study had globally low myocardial perfusion at stress and absence of splenic switch-off, hence absence of adenosine effect is not the main explanation to the results of this paper. In Paper II, absence of adenosine effect should not affect the results, since the comparison of reconstruction and post-

processing parameters was done within the same examination. Furthermore, in Paper V, the adenosine was infused at a constant dose of 140 µg/kg/min to avoid bias in the results due to different adenosine doses between examinations.

In papers I and III, only the highest degree of coronary artery stenosis in each vessel territory was included in the analyses and the effect of serial stenoses and collateral blood supply was not assessed. Furthermore, invasive functional evaluation was lacking in several patients. Hence, the functional significance of the coronary artery stenoses and microvascular dysfunction assessed from ICA was not explored in these papers.

In Paper II, different reconstruction and post-processing parameters were changed one by one and compared with the standard parameters. Hence, the effect of changing several parameters at once was not investigated. Myocardial perfusion quantification at high perfusion levels might differ between radiopharmaceuticals with different extraction fractions[117]. However, only one radiopharmaceutical (^{13}N ammonia) was investigated in Paper II. Furthermore, previous studies have shown that choice of software solutions might affect myocardial perfusion quantification[118]. However, the results of Paper II can only be applied to using the software Carimas.

In Paper V, the first examination of the pre-menopausal women was always conducted in the EFP. Therefore, the women were familiar with the examination procedure at the second examination, which might decrease anxiety during the examination. Hence, the order of the examinations might contribute to the decrease in perfusion at stress in the MLP. However, the absolute hormone levels can vary between different menstrual cycles in the same woman and the study aimed to investigate the variations in myocardial perfusion during one menstrual cycle.

Confounders not accounted for in the statistical analyses due to lack of power might influence the results of this thesis. For instance, in Paper I, only hypertension, diabetes and smoking were added to the mixed model, but other comorbidities and medications might also influence myocardial perfusion. In Paper IV, it would have been of interest to include exercise habits of the patients, but this data was not collected. In Paper V, the strict inclusion criteria of the participants aimed to eliminate several confounders, but other factors such as level of exercise, amount of sleep and stress levels might affect the results.

Chapter 6

Conclusions

The major conclusions of the five papers are as follows:

Paper I Sex, age, diabetes, hypertension and smoking affect myocardial perfusion independently of degree of coronary artery stenosis in patients with suspected CCS. Therefore, these factors need to be considered when assessing the significance of reduced myocardial perfusion.

Paper II The addition of ToF, position and size of blood pool VOI and choice of compartment model affect myocardial perfusion quantification more than choice of time-frame schemes and reconstruction algorithms. Therefore, these parameters should be kept constant when comparing examinations.

Paper III Visual assessment of degree of coronary artery stenosis on ICA has limited diagnostic accuracy for detecting reduced myocardial perfusion, as measured by qFPP CMR.

Paper IV Change in myocardial perfusion after revascularization does not correlate with change in VO_2 peak in patients with CCS, regardless of the baseline level of myocardial perfusion prior to revascularization.

Paper V Serum estradiol levels may influence myocardial perfusion at stress in healthy pre- and post-menopausal women.

Chapter 7

Future perspectives

The results of this thesis give rise to several new research questions to be answered. As paper I showed, together with several previous studies[14, 15, 119], there is a sex difference in myocardial perfusion. Paper V aimed to contribute to the understanding of the physiological mechanisms behind the higher myocardial perfusion in women. However, to establish how the sex differences should be accounted for in the clinical work to improve outcome for patients, further research to understand the mechanism behind the sex differences is needed.

In paper IV, only VO_2 peak was included in the analyses. There might be other CPET variables associating with change in myocardial perfusion, and investigating these parameters might contribute to the understanding of the effect of revascularization on cardiopulmonary capacity.

As mentioned in the introduction and limitations section, the absence of adenosine effect can lead to false low myocardial perfusion at stress. Adenosine dose can safely be increased up to 210 µg/kg/min[53] and Brown et al recently showed that 210 µg/kg/min does increase myocardial perfusion at stress in patients with reduced ejection fraction[54]. Since absence of adenosine effect might lead to false negative examination results when using modalities depicting the relative perfusion distribution of the myocardium, like cardiac single photon emission computed tomography, the understanding of the effect of adenosine on hyperemia needs to be further explored. A current clinical trial, the HYPER trial, at the Department of Clinical Physiology, Skåne University Hospital, Lund, aims to investigate the effect of adenosine dose on the hyperemic response in the myocardium in relation to anthropometric variables and comorbidities. Patients and sex- and age-matched healthy volunteers undergo two adenosine stress perfusion acquisitions during the same qFPP CMR examination. The participants are randomized to start with either standard (140 µg/kg/min) or high (210 µg/kg/min) dose adenosine. Since caffeine is an antagonist to adenosine, serum caffeine levels are measured at the study visit.

To conclude, future research should explore how the modalities for quantitative myocardial perfusion assessment should be implemented to maximize the outcome for patients and increase our understanding of human physiology.

References

[1] Marios Loukas, Christopher Groat, Rajkamal Khangura, Deyzi Gueorguieva Owens, and Robert H Anderson. The normal and abnormal anatomy of the coronary arteries. *Clinical Anatomy: The Official Journal of the American Association of Clinical Anatomists and the British Association of Clinical Anatomists*, 22(1):114–128, 2009.

[2] Arthur C Guyton and John E Hall. Guyton and hall textbook of medical physiology. *Elsevier*, 2011.

[3] World Health Organization. Global status report on noncommunicable diseases 2014. page 176, 2014. ISSN 1475-5785. doi: ISBN9789241564854. URL `http://www.who.int/nmh/publications/ncd-status-report-2014/en/`.

[4] Christiaan Vrints, Felicita Andreotti, Konstantinos C Koskinas, Xavier Rossello, Marianna Adamo, James Ainslie, et al. 2024 esc guidelines for the management of chronic coronary syndromes: developed by the task force for the management of chronic coronary syndromes of the european society of cardiology (esc) endorsed by the european association for cardio-thoracic surgery (eacts). *European heart journal*, 45(36):3415–3537, 2024.

[5] Richard W Nesto and Glen J Kowalchuk. The ischemic cascade: temporal sequence of hemodynamic, electrocardiographic and symptomatic expressions of ischemia. *The American journal of cardiology*, 59(7):C23–C30, 1987.

[6] Thor Edvardsen, Federico M Asch, Brian Davidson, Victoria Delgado, Anthony DeMaria, Vasken Dilsizian, et al. Non-invasive imaging in coronary syndromes: recommendations of the european association of cardiovascular imaging and the american society of echocardiography, in collaboration with the american society of nuclear cardiology, society of cardiovascular computed tomography, and society for cardiovascular magnetic resonance. *European Heart Journal-Cardiovascular Imaging*, 23(2):e6–e33, 2022.

[7] Carl W White, Creighton B Wright, Donald B Doty, Loren F Hiratza, Charles L Eastham, David G Harrison, et al. Does visual interpretation of the coronary arteriogram predict the physiologic importance of a coronary stenosis? *New England Journal of Medicine*, 310(13):819–824, 1984.

[8] Peter Vasko, Joakim Alfredsson, Maria Bäck, Lars Dahlbom, David Erlinge, Mira Ernkvist, et al. Swedeheart annual report 2023.

Upps. Clin. Res. Cent, page 144, 2023. URL https://www.ucr.uu.se/swedeheart/dokument-sh/arsrapporter-sh/arsrapport-2023/01-swedeheart-annual-report-2023-english.

[9] Franz-Josef Neumann, Miguel Sousa-Uva, Anders Ahlsson, Fernando Alfonso, Adrian P Banning, Umberto Benedetto, et al. 2018 esc/eacts guidelines on myocardial revascularization. *European heart journal*, 40(2):87–165, 2019.

[10] Ana G Almeida, Julia Grapsa, Alessia Gimelli, Chiara Bucciarelli-Ducci, Bernhard Gerber, Nina Ajmone-Marsan, et al. Cardiovascular multimodality imaging in women: a scientific statement of the european association of cardiovascular imaging of the european society of cardiology. *European Heart Journal - Cardiovascular Imaging*, 25(4):e116–e136, 01 2024. ISSN 2047-2404.

[11] Sonia S Anand, Shofiqul Islam, Annika Rosengren, Maria Grazia Franzosi, Krisela Steyn, Afzal Hussein Yusufali, et al. Risk factors for myocardial infarction in women and men: insights from the interheart study. *European heart journal*, 29 (7):932–940, 2008.

[12] Harmony R Reynolds, Leslee J Shaw, James K Min, John A Spertus, Bernard R Chaitman, Daniel S Berman, et al. Association of sex with severity of coronary artery disease, ischemia, and symptom burden in patients with moderate or severe ischemia: secondary analysis of the ischemia randomized clinical trial. *JAMA cardiology*, 5(7):773–786, 2020.

[13] Steven E Reis, Richard Holubkov, AJ Conrad Smith, Sheryl F Kelsey, Barry L Sharaf, Nathaniel Reichek, et al. Coronary microvascular dysfunction is highly prevalent in women with chest pain in the absence of coronary artery disease: results from the nhlbi wise study. *American heart journal*, 141(5):735–741, 2001.

[14] Jannike Nickander, Raquel Themudo, Andreas Sigfridsson, Hui Xue, Peter Kellman, and Martin Ugander. Females have higher myocardial perfusion, blood volume and extracellular volume compared to males–an adenosine stress cardiovascular magnetic resonance study. *Scientific reports*, 10(1):10380, 2020.

[15] Louise AE Brown, Gaurav S Gulsin, Sebastian C Onciul, David A Broadbent, Jian L Yeo, Alice L Wood, et al. Sex-and age-specific normal values for automated quantitative pixel-wise myocardial perfusion cardiovascular magnetic resonance. *European Heart Journal-Cardiovascular Imaging*, 24(4):426–434, 2023.

[16] Ronée E Harvey, Kirsten E Coffman, and Virginia M Miller. Women-specific factors to consider in risk, diagnosis and treatment of cardiovascular disease. *Women's Health*, 11(2):239–257, 2015.

[17] C Noel Bairey Merz, Marian B Olson, Candace McClure, Yu-Ching Yang, James Symons, George Sopko, et al. A randomized controlled trial of low-dose hormone therapy on myocardial ischemia in postmenopausal women with no obstructive coronary artery disease: Results from the national institutes of health/national heart, lung, and blood institute–sponsored women's ischemia syndrome evaluation (wise). *American heart journal*, 159(6):987–e1, 2010.

[18] Juhani Knuuti, Riikka Kalliokoski, Tuula Janatuinen, Jarna Hannukainen, Kari K Kalliokoski, Juha Koskenvuo, et al. Effect of estradiol-drospirenone hormone treatment on myocardial perfusion reserve in postmenopausal women with angina pectoris. *The American journal of cardiology*, 99(12):1648–1652, 2007.

[19] Paula S McKinley, Arlene R King, Peter A Shapiro, Iordan Slavov, Yixin Fang, Ivy S Chen, et al. The impact of menstrual cycle phase on cardiac autonomic regulation. *Psychophysiology*, 46(4):904–911, 2009.

[20] Jason R Carter, Qi Fu, Christopher T Minson, and Michael J Joyner. Ovarian cycle and sympathoexcitation in premenopausal women. *Hypertension*, 61(2): 395–399, 2013.

[21] Kumiko Hirata, Kenei Shimada, Hiroyuki Watanabe, Takashi Muro, Minoru Yoshiyama, Kazuhide Takeuchi, et al. Modulation of coronary flow velocity reserve by gender, menstrual cycle and hormone replacement therapy. *Journal of the American College of Cardiology*, 38(7):1879–1884, 2001.

[22] Katja M Schmalenberger, Hafsah A Tauseef, Jordan C Barone, Sarah A Owens, Lynne Lieberman, Marc N Jarczok, et al. How to study the menstrual cycle: Practical tools and recommendations. *Psychoneuroendocrinology*, 123:104895, 2021.

[23] Marc Dewey, Maria Siebes, Marc Kachelrieß, Klaus F Kofoed, Pál Maurovich-Horvat, Konstantin Nikolaou, et al. Clinical quantitative cardiac imaging for the assessment of myocardial ischaemia. *Nature Reviews Cardiology*, 17(7):427–450, 2020.

[24] Juhani Knuuti, Haitham Ballo, Luis Eduardo Juarez-Orozco, Antti Saraste, Philippe Kolh, Anne Wilhelmina Saskia Rutjes, et al. The performance of non-invasive tests to rule-in and rule-out significant coronary artery stenosis in patients with stable angina: a meta-analysis focused on post-test disease probability. *European Heart Journal*, 39(35):3322–3330, 05 2018. ISSN 0195-668X.

[25] Ami E Iskandrian and Ernest V Garcia. Nuclear cardiac imaging: Principles and applications. *Oxford University Press, USA*, 2008.

[26] Eugene Lin and Abass Alavi. Pet and pet/ct. *Thieme medical publisher inc*, 2009.

[27] Jamshid Maddahi and René R.S. Packard. Cardiac pet perfusion tracers: Current status and future directions. *Seminars in Nuclear Medicine*, 44(5):333–343, 2014. ISSN 0001-2998.

[28] Roberto Sciagrà, Mark Lubberink, Fabien Hyafil, Antti Saraste, Riemer Slart, Denis Agostini, et al. Eanm procedural guidelines for pet/ct quantitative myocardial perfusion imaging. *European Journal of Nuclear Medicine and Molecular Imaging*, 48:1–30, 04 2021.

[29] James A Case, Robert A deKemp, Piotr J Slomka, Mark F Smith, Gary V Heller, and Manuel D Cerqueira. Status of cardiovascular pet radiation exposure and strategies for reduction: An information statement from the cardiovascular pet task force. *Journal of Nuclear Cardiology*, 24(4):1427–1439, 2017.

[30] Harrison H Barrett, Timothy White, and Lucas C Parra. List-mode likelihood. *Journal of the Optical Society of America A*, 14(11):2914–2923, 1997.

[31] Michel M. Ter-Pogossian, David C. Ficke, Mikio Yamamoto, and John T. Hood. Super pett i: A positron emission tomograph utilizing photon time-of-flight information. *IEEE Transactions on Medical Imaging*, 1(3):179–187, 1982. doi: 10.1109/TMI.1982.4307570.

[32] Suleman Surti. Update on time-of-flight pet imaging. *Journal of Nuclear Medicine*, 56(1):98–105, 2015.

[33] Masaya Suda, Masahisa Onoguchi, Takeshi Tomiyama, Keiichi Ishihara, Naoto Takahashi, Minoru Sakurai, et al. The reproducibility of time-of-flight pet and conventional pet for the quantification of myocardial blood flow and coronary flow reserve with 13n-ammonia. *Journal of Nuclear Cardiology*, 23(3):457–472, 2016.

[34] Andres F Vasquez, Nils P Johnson, and K Lance Gould. Variation in quantitative myocardial perfusion due to arterial input selection. *JACC: Cardiovascular Imaging*, 6(5):559–568, 2013.

[35] Ran Klein, Rob SB Beanlands, and Robert A Dekemp. Quantification of myocardial blood flow and flow reserve: technical aspects. *Journal of nuclear cardiology*, 17(4):555–570, 2010.

[36] Timothy R DeGrado, Michael W Hanson, Timothy G Turkington, David M Delong, Damian A Brezinski, Jean-Paul Vallée, et al. Estimation of myocardial blood flow for longitudinal studies with 13n-labeled ammonia and positron emission tomography. *Journal of Nuclear Cardiology*, 3(6):494–507, 1996.

[37] Janine Krivokapich, GT Smith, Sung-Cheng Huang, EJ Hoffman, O Ratib, ME Phelps, et al. 13n ammonia myocardial imaging at rest and with exercise in normal volunteers. quantification of absolute myocardial perfusion with dynamic positron emission tomography. *Circulation*, 80(5):1328–1337, 1989.

[38] Gary D Hutchins, Markus Schwaiger, Karen C Rosenspire, Janine Krivokapich, Heinrich Schelbert, and David E Kuhl. Noninvasive quantification of regional blood flow in the human heart using n-13 ammonia and dynamic positron emission tomographic imaging. *Journal of the American College of Cardiology*, 15(5):1032–1042, 1990.

[39] Aliasghar Khorsand, Senta Graf, Christian Pirich, Otto Muzik, Kurt Kletter, Robert Dudczak, et al. Assessment of myocardial perfusion by dynamic n-13 ammonia pet imaging: comparison of 2 tracer kinetic models. *Journal of nuclear cardiology*, 12(4):410–417, 2005.

[40] Donald W. McRobbie, Elizabeth A. Moore, Martin J. Graves, and Martin R. Prince. Mri from picture to proton, third edition. *Cambridge University Press*, 2017.

[41] Henrik Engblom, Hui Xue, Shahnaz Akil, Marcus Carlsson, Cecilia Hindorf, Jenny Oddstig, et al. Fully quantitative cardiovascular magnetic resonance myocardial perfusion ready for clinical use: a comparison between cardiovascular magnetic resonance imaging and positron emission tomography. *Journal of Cardiovascular Magnetic Resonance*, 19(1):78, 2016.

[42] Hans H Schild. Mri made easy. *Schering AG*, 1990.

[43] Christopher M Kramer, Jörg Barkhausen, Chiara Bucciarelli-Ducci, Scott D Flamm, Raymond J Kim, and Eike Nagel. Standardized cardiovascular magnetic resonance imaging (cmr) protocols: 2020 update. *Journal of Cardiovascular Magnetic Resonance*, 22(1):17, 2020.

[44] Hakan Arheden, Maythem Saeed, Charles B Higgins, Dong-Wei Gao, Jens Bremerich, Rolf Wyttenbach, et al. Measurement of the distribution volume of gadopentetate dimeglumine at echo-planar mr imaging to quantify myocardial infarction: comparison with 99mtc-dtpa autoradiography in rats. *Radiology*, 211 (3):698–708, 1999.

[45] Maythem Saeed, Michael F. Wendland, Takayuki Masui, and Charles B. Higgins. Reperfused myocardial infarctions on T1- and susceptibility-enhanced MRI: Evidence for loss of compartmentalization of contrast media. *Magnetic Resonance in Medicine*, 31(1):31–39, 1994. ISSN 15222594.

[46] Raymond J Kim, David S Fieno, Todd B Parrish, Kathleen Harris, Enn-Ling Chen, Orlando Simonetti, et al. Relationship of mri delayed contrast enhancement to irreversible injury, infarct age, and contractile function. *Circulation*, 100(19): 1992–2002, 1999.

[47] Tushar Kotecha, Ana Martinez-Naharro, Michele Boldrini, Daniel Knight, Philip Hawkins, Sundeep Kalra, et al. Automated pixel-wise quantitative myocardial perfusion mapping by cmr to detect obstructive coronary artery disease and coronary microvascular dysfunction: validation against invasive coronary physiology. *JACC: Cardiovascular Imaging*, 12(10):1958–1969, 2019.

[48] Peter Kellman, Michael S Hansen, Sonia Nielles-Vallespin, Jannike Nickander, Raquel Themudo, Martin Ugander, et al. Myocardial perfusion cardiovascular magnetic resonance: optimized dual sequence and reconstruction for quantification. *Journal of Cardiovascular Magnetic Resonance*, 19(1):43, 2016.

[49] Hui Xue, Michael S Hansen, Sonia Nielles-Vallespin, Andrew E Arai, and Peter Kellman. Inline quantitative myocardial perfusion flow mapping. *Journal of Cardiovascular Magnetic Resonance*, 18(1):W8, 2016.

[50] Henrik Engblom, Ellen Ostenfeld, Marcus Carlsson, Julius Åkesson, Anthony H Aletras, Hui Xue, et al. Diagnostic confidence with quantitative cardiovascular magnetic resonance perfusion mapping increases with increased coverage of the left ventricle. *Journal of Cardiovascular Magnetic Resonance*, 26(1):101007, 2024.

[51] Michael Schacht Hansen and Thomas Sangild Sørensen. Gadgetron: an open source framework for medical image reconstruction. *Magnetic resonance in medicine*, 69(6):1768–1776, 2013.

[52] James Bassingthwaighte, CY Wang, and IS Chan. Blood-tissue exchange via transport and transformation by capillary endothelial cells. *Circulation research*, 65(4):997–1020, 1989.

[53] Theodoros D Karamitsos, Ntobeko AB Ntusi, Jane M Francis, Cameron J Holloway, Saul G Myerson, and Stefan Neubauer. Feasibility and safety of high-dose adenosine perfusion cardiovascular magnetic resonance. *Journal of Cardiovascular Magnetic Resonance*, 12:1–8, 2010.

[54] Louise AE Brown, Christopher ED Saunderson, Arka Das, Thomas Craven, Eylem Levelt, Kristopher D Knott, et al. A comparison of standard and high dose adenosine protocols in routine vasodilator stress cardiovascular magnetic resonance: dosage affects hyperaemic myocardial blood flow in patients with severe left ventricular systolic impairment. *Journal of Cardiovascular Magnetic Resonance*, 23(1):37, 2021.

[55] Marcus Carlsson, Jonas Jögi, Karin Markenroth Bloch, Bo Hedén, Ulf Ekelund, Freddy Ståhlberg, et al. Submaximal adenosine-induced coronary hyperaemia with 12 h caffeine abstinence: implications for clinical adenosine perfusion imaging tests. *Clinical physiology and functional imaging*, 35(1):49–56, 2015.

[56] Eliana Reyes, Chee Y Loong, Mark Harbinson, Jackie Donovan, Constantinos Anagnostopoulos, and S Richard Underwood. High-dose adenosine overcomes the attenuation of myocardial perfusion reserve caused by caffeine. *Journal of the American College of Cardiology*, 52(24):2008–2016, 2008.

[57] Robert F Wilson, Keith Wyche, Betsy V Christensen, Steven Zimmer, and David D Laxson. Effects of adenosine on human coronary arterial circulation. *Circulation*, 82(5):1595–1606, 1990.

[58] Tushar Kotecha, Juan Manuel Monteagudo, Ana Martinez-Naharro, Liza Chacko, James Brown, Daniel Knight, et al. Quantitative cardiovascular magnetic resonance myocardial perfusion mapping to assess hyperaemic response to adenosine stress. *European Heart Journal-Cardiovascular Imaging*, 22(3):273–281, 2021.

[59] Charlotte Manisty, David P Ripley, Anna S Herrey, Gabriella Captur, Timothy C Wong, Steffen E Petersen, et al. Splenic switch-off: a tool to assess stress adequacy in adenosine perfusion cardiac mr imaging. *Radiology*, 276(3):732–740, 2015.

[60] Viktor Kočka. The coronary angiography–an old-timer in great shape. *Cor et vasa*, 57(6):e419–e424, 2015.

[61] David Corcoran, Colin Berry, and Keith Oldroyd. Current frontiers in the clinical research of coronary physiology. *Interventional Cardiology*, 7(1):97, 2015.

[62] Gary J Balady, Ross Arena, Kathy Sietsema, Jonathan Myers, Lola Coke, Gerald F Fletcher, et al. Clinician's guide to cardiopulmonary exercise testing in adults: a scientific statement from the american heart association. *Circulation*, 122(2):191–225, 2010.

[63] Karlman Wasserman, James E. Hansen, Darryl Y Sue, William W. Stringer, Kathy E Sietsema, Xing-Guo Sun, et al. Principles of exercise testing and interpretation: Including pathophysiology and clinical applications. *Lippincott Williams and Wilkins*, 2011.

[64] Sven Gläser, Beate Koch, Till Ittermann, Christoph Schäper, Marcus Dörr, Stephan B Felix, et al. Influence of age, sex, body size, smoking, and β blockade on key gas exchange exercise parameters in an adult population. *European Journal of Preventive Cardiology*, 17(4):469–476, 2010.

[65] Bai-Chin Lee, Ssu-Yuan Chen, Hsiu-Ching Hsu, Mao-Yuan Marine Su, Yen-Wen Wu, Kuo-Liong Chien, et al. Effect of cardiac rehabilitation on myocardial perfusion reserve in postinfarction patients. *The American journal of cardiology*, 101 (10):1395–1402, 2008.

[66] Luc Vanhees, Robert Fagard, Lutgarde Thijs, Jan Staessen, and Antoon Amery. Prognostic significance of peak exercise capacity in patients with coronary artery disease. *Journal of the American College of Cardiology*, 23(2):358–363, 1994.

[67] Jonathan Myers, Manish Prakash, Victor Froelicher, Dat Do, Sara Partington, and J Edwin Atwood. Exercise capacity and mortality among men referred for exercise testing. *New England journal of medicine*, 346(11):793–801, 2002.

[68] T Kavanagh, DJ Mertens, and LF Hamm. Peak oxygen intake and cardiac mortality in women referred for cardiac rehabilitation. *ACC Current Journal Review*, 13(4):12, 2004.

[69] Anvesha Singh, Michael Jerosch-Herold, Soliana Bekele, Anna-Marie Marsh, John McAdam, John P Greenwood, et al. Determinants of exercise capacity and myocardial perfusion reserve in asymptomatic patients with aortic stenosis. *Cardiovascular Imaging*, 13(1_Part_1):178–180, 2020.

[70] Gaurav S Gulsin, Joseph Henson, Emer M Brady, Jack A Sargeant, Emma G Wilmot, Lavanya Athithan, et al. Cardiovascular determinants of aerobic exercise capacity in adults with type 2 diabetes. *Diabetes Care*, 43(9):2248–2256, 2020.

[71] Abhishek Dattani, Benjamin A Marrow, Gaurav S Gulsin, Jian L Yeo, Amitha Puranik, Emer M Brady, et al. Association between coronary microvascular dysfunction and exercise capacity in dilated cardiomyopathy. *Journal of Cardiovascular Magnetic Resonance*, 26(2):101108, 2024.

[72] Manuel D Cerqueira, Neil J Weissman, Vasken Dilsizian, Alice K Jacobs, Sanjiv Kaul, Warren K Laskey, et al. Standardized myocardial segmentation and nomenclature for tomographic imaging of the heart: a statement for healthcare professionals from the cardiac imaging committee of the council on clinical cardiology of the american heart association. *Circulation*, 105(4):539–542, 2002.

[73] Jamil Tajik and James Seward. Standardized nomenclature and anatomic basis for regional tomographic analysis of the heart. *Mayo Clinic proceedings. Mayo Clinic*, 56:479–97, 09 1981.

[74] Donna M Gallik, Steve D Obermueller, Udaya S Swarna, Gerald W Guidry, John J Mahmarian, and Mario S Verani. Simultaneous assessment of myocardial perfusion and left ventricular function during transient coronary occlusion. *Journal of the American College of Cardiology*, 25(7):1529–1538, 1995.

[75] Naresh C. Gupta, Dennis Esterbrooks, Syed Mohiuddin, Dan Hilleman, John Sunderland, Chyng Y. Shiue, et al. Adenosine in myocardial perfusion imaging using positron emission tomography. *American Heart Journal*, 122(1, Part 1): 293–301, 1991. ISSN 0002-8703.

[76] H Malcolm Hudson and Richard S Larkin. Accelerated image reconstruction using ordered subsets of projection data. *IEEE transactions on medical imaging*, 13(4): 601–609, 1994.

[77] Oona Rainio, Chunlei Han, Jarmo Teuho, Sergey V Nesterov, Vesa Oikonen, Sauli Piirola, et al. Carimas: an extensive medical imaging data processing tool for research. *Journal of Digital Imaging*, 36(4):1885–1893, 2023.

[78] C.-T. Chen, V.E. Johnson, W.H. Wong, X. Hu, and C.E. Metz. Bayesian image reconstruction in positron emission tomography. *IEEE Transactions on Nuclear Science*, 37(2):636–641, 1990. doi: 10.1109/23.106690.

[79] Steve Ross. Q.clear. *GE health care*, 2014.

[80] Kelvin Chow, Genevieve Hayes, Jacqueline A Flewitt, Patricia Feuchter, Carmen Lydell, Andrew Howarth, et al. Improved accuracy and precision with three-parameter simultaneous myocardial t1 and t2 mapping using multiparametric sasha. *Magnetic resonance in medicine*, 87(6):2775–2791, 2022.

[81] Orlando P Simonetti, Raymond J Kim, David S Fieno, Hanns B Hillenbrand, Edwin Wu, Jeffrey M Bundy, et al. An improved mr imaging technique for the visualization of myocardial infarction. *Radiology*, 218(1):215–223, 2001.

[82] Einar Heiberg, Jane Sjögren, Martin Ugander, Marcus Carlsson, Henrik Engblom, and Håkan Arheden. Design and validation of segment-freely available software for cardiovascular image analysis. *BMC medical imaging*, 10(1):1, 2010.

[83] Kristopher D Knott, Andreas Seraphim, Joao B Augusto, Hui Xue, Liza Chacko, Nay Aung, et al. The prognostic significance of quantitative myocardial perfusion: an artificial intelligence–based approach using perfusion mapping. *Circulation*, 141(16):1282–1291, 2020.

[84] Jeanette Schulz-Menger, David A Bluemke, Jens Bremerich, Scott D Flamm, Mark A Fogel, Matthias G Friedrich, et al. Standardized image interpretation and post-processing in cardiovascular magnetic resonance-2020 update: Society for cardiovascular magnetic resonance (scmr): Board of trustees task force on

standardized post-processing. *Journal of cardiovascular magnetic resonance*, 22 (1):19, 2020.

[85] Henrik Engblom, Jane Tufvesson, Robert Jablonowski, Marcus Carlsson, Anthony H Aletras, Pavel Hoffmann, et al. A new automatic algorithm for quantification of myocardial infarction imaged by late gadolinium enhancement cardiovascular magnetic resonance: experimental validation and comparison to expert delineations in multi-center, multi-vendor patient data. *Journal of Cardiovascular Magnetic Resonance*, 18(1):27, 2016.

[86] J Martin Bland and DouglasG Altman. Statistical methods for assessing agreement between two methods of clinical measurement. *The lancet*, 327(8476):307–310, 1986.

[87] Christel H Kamani, Louise Brown, Thomas Anderton, Raluca Tomoaia, Chin Soo, Gaurav S Gulsin, et al. Normal values of high-resolution transmural perfusion distribution metrics for automated quantitative pixel-wise myocardial perfusion cmr. *Journal of Cardiovascular Magnetic Resonance*, page 101927, 2025.

[88] Joo Myung Lee, Chee Hae Kim, Bon-Kwon Koo, Doyeon Hwang, Jonghanne Park, Jinlong Zhang, et al. Integrated myocardial perfusion imaging diagnostics improve detection of functionally significant coronary artery stenosis by 13n-ammonia positron emission tomography. *Circulation: Cardiovascular Imaging*, 9(9):e004768, 2016.

[89] Rita Pingree, Susanne Markendorf, Dimitrios Moysidis, Christoph Ryffel, Magdalena Stuetz, Raffael Ghenzi, et al. Myocardial blood flow reference values for 13n-ammonia pet myocardial perfusion imaging in patients without flow-limiting coronary artery disease. *European Journal of Nuclear Medicine and Molecular Imaging*, pages 1–11, 2025.

[90] Ibrahim Danad, Valtteri Uusitalo, Tanja Kero, Antti Saraste, Pieter G Raijmakers, Adriaan A Lammertsma, et al. Quantitative assessment of myocardial perfusion in the detection of significant coronary artery disease: cutoff values and diagnostic accuracy of quantitative [15o] h2o pet imaging. *Journal of the American College of Cardiology*, 64(14):1464–1475, 2014.

[91] David M Gilligan, Arshed A Quyyumi, and RO Cannon 3rd. Effects of physiological levels of estrogen on coronary vasomotor function in postmenopausal women. *Circulation*, 89(6):2545–2551, 1994.

[92] Chutima Rattanasopa, Sukanya Phungphong, Jonggonnee Wattanapermpool, and Tepmanas Bupha-Intr. Significant role of estrogen in maintaining cardiac mitochondrial functions. *The Journal of steroid biochemistry and molecular biology*, 147:1–9, 2015.

[93] Natalie Burkard, Tatjana Williams, Martin Czolbe, Nadja Blömer, Franziska Panther, Martin Link, et al. Conditional overexpression of neuronal nitric oxide synthase is cardioprotective in ischemia/reperfusion. *Circulation*, 122(16):1588–1603, 2010.

[94] Sandy Goyette, Tulika Mishra, Farah Raza, Zahra Naqvi, Sarah Khan, Abrar Khan, et al. Menstruation-related angina—the wee hours. *International Journal of Angiology*, 33(04):229–236, 2024.

[95] GW Lloyd, NR Patel, E McGing, AF Cooper, D Brennand-Roper, and G Jackson. Does angina vary with the menstrual cycle in women with premenopausal coronary artery disease? *Heart*, 84(2):189–192, 2000.

[96] C Noel Bairey Merz, B Delia Johnson, Barry L Sharaf, Vera Bittner, Sarah L Berga, Glenn D Braunstein, et al. Hypoestrogenemia of hypothalamic origin and coronary artery disease in premenopausal women: a report from the nhlbi-sponsored wise study. *Journal of the American College of Cardiology*, 41(3): 413–419, 2003.

[97] Andreas M Zeiher, Volker Schachinger, and Jan Minners. Long-term cigarette smoking impairs endothelium-dependent coronary arterial vasodilator function. *Circulation*, 92(5):1094–1100, 1995.

[98] Marcelo F Di Carli, James Janisse, Joel Ager, and George Grunberger. Role of chronic hyperglycemia in the pathogenesis of coronary microvascular dysfunction in diabetes. *Journal of the American College of Cardiology*, 41(8):1387–1393, 2003.

[99] John E Brush Jr, Richard O Cannon III, William H Schenke, Robert O Bonow, Martin B Leon, Barry J Maron, et al. Angina due to coronary microvascular disease in hypertensive patients without left ventricular hypertrophy. *New England Journal of Medicine*, 319(20):1302–1307, 1988.

[100] Lasse Jespersen, Anders Hvelplund, Steen Z Abildstrøm, Frants Pedersen, Søren Galatius, Jan K Madsen, et al. Stable angina pectoris with no obstructive coronary artery disease is associated with increased risks of major adverse cardiovascular events. *European heart journal*, 33(6):734–744, 2012.

[101] Jaskanwal D Sara, R Jay Widmer, Yasushi Matsuzawa, Ryan J Lennon, Lilach O Lerman, and Amir Lerman. Prevalence of coronary microvascular dysfunction among patients with chest pain and nonobstructive coronary artery disease. *Cardiovascular Interventions*, 8(11):1445–1453, 2015.

[102] Tara L Sedlak, May Lee, Mona Izadnegahdar, C Noel Bairey Merz, Min Gao, and Karin H Humphries. Sex differences in clinical outcomes in patients with stable angina and no obstructive coronary artery disease. *American heart journal*, 166 (1):38–44, 2013.

[103] Thomas J Ford, Bethany Stanley, Richard Good, Paul Rocchiccioli, Margaret McEntegart, Stuart Watkins, et al. Stratified medical therapy using invasive coronary function testing in angina: the cormica trial. *Journal of the American College of Cardiology*, 72(23 Part A):2841–2855, 2018.

[104] Shahnaz Akil, Fredrik Hedeer, Jenny Oddstig, Thomas Olsson, Jonas Jögi, David Erlinge, et al. Appropriate coronary revascularization can be accomplished if

myocardial perfusion is quantified by positron emission tomography prior to treatment decision. *Journal of Nuclear Cardiology*, 28(4):1664–1672, 2021.

[105] David J Maron, Judith S Hochman, Harmony R Reynolds, Sripal Bangalore, Sean M O'Brien, William E Boden, et al. Initial invasive or conservative strategy for stable coronary disease. *New England Journal of Medicine*, 382(15):1395–1407, 2020.

[106] William E Boden, Robert A O'Rourke, Koon K Teo, Pamela M Hartigan, David J Maron, William J Kostuk, et al. Optimal medical therapy with or without pci for stable coronary disease. *New England journal of medicine*, 356(15):1503–1516, 2007.

[107] Ibrahim Danad, Jackie Szymonifka, Jos WR Twisk, Bjarne L Norgaard, Christopher K Zarins, Paul Knaapen, et al. Diagnostic performance of cardiac imaging methods to diagnose ischaemia-causing coronary artery disease when directly compared with fractional flow reserve as a reference standard: a meta-analysis. *European heart journal*, 38(13):991–998, 2017.

[108] Michael Fiechter, Jelena R Ghadri, Cathérine Gebhard, Tobias A Fuchs, Aju P Pazhenkottil, Rene N Nkoulou, et al. Diagnostic value of 13n-ammonia myocardial perfusion pet: added value of myocardial flow reserve. *Journal of Nuclear Medicine*, 53(8):1230–1234, 2012.

[109] Masanao Naya, Venkatesh L Murthy, Viviany R Taqueti, Courtney R Foster, Josh Klein, Mariya Garber, et al. Preserved coronary flow reserve effectively excludes high-risk coronary artery disease on angiography. *Journal of Nuclear Medicine*, 55(2):248–255, 2014.

[110] Ankur Gupta, Viviany R Taqueti, Tim P van de Hoef, Navkaranbir S Bajaj, Paco E Bravo, Venkatesh L Murthy, et al. Integrated noninvasive physiological assessment of coronary circulatory function and impact on cardiovascular mortality in patients with stable coronary artery disease. *Circulation*, 136(24):2325–2336, 2017.

[111] John P Greenwood, David P Ripley, Colin Berry, Gerry P McCann, Sven Plein, Chiara Bucciarelli-Ducci, et al. Effect of care guided by cardiovascular magnetic resonance, myocardial perfusion scintigraphy, or nice guidelines on subsequent unnecessary angiography rates: the ce-marc 2 randomized clinical trial. *Jama*, 316(10):1051–1060, 2016.

[112] Jane S Skinner, Liam Smeeth, Jason M Kendall, Philip C Adams, and Adam Timmis. Nice guidance. chest pain of recent onset: assessment and diagnosis of recent onset chest pain or discomfort of suspected cardiac origin. *Heart*, 96(12): 974–978, 2010.

[113] Jose Gavara, Nerea Perez, Victor Marcos-Garces, Jose V Monmeneu, Maria P Lopez-Lereu, Cesar Rios-Navarro, et al. Combined assessment of stress cardiovascular magnetic resonance and angiography to predict the effect of revascularization in chronic coronary syndrome patients. *European Journal of Preventive Cardiology*, 29(2):407–416, 2022.

[114] Christopher A Rajkumar, Michael J Foley, Fiyyaz Ahmed-Jushuf, Alexandra N Nowbar, Florentina A Simader, John R Davies, et al. A placebo-controlled trial of percutaneous coronary intervention for stable angina. *New England Journal of Medicine*, 389(25):2319–2330, 2023.

[115] John A Spertus, Philip G Jones, David J Maron, Sean M O'Brien, Harmony R Reynolds, Yves Rosenberg, et al. Health-status outcomes with invasive or conservative care in coronary disease. *New England Journal of Medicine*, 382(15): 1408–1419, 2020.

[116] Rasha Al-Lamee, David Thompson, Hakim-Moulay Dehbi, Sayan Sen, Kare Tang, John Davies, et al. Percutaneous coronary intervention in stable angina (orbita): a double-blind, randomised controlled trial. *The Lancet*, 391(10115):31–40, 2018.

[117] Georges El Fakhri, Arash Kardan, Arkadiusz Sitek, Sharmila Dorbala, Nathalie Abi-Hatem, Youmna Lahoud, et al. Reproducibility and accuracy of quantitative myocardial blood flow assessment with 82rb pet: comparison with 13n-ammonia pet. *Journal of Nuclear Medicine*, 50(7):1062–1071, 2009.

[118] Andrea G Monroy-Gonzalez, Luis Eduardo Juarez-Orozco, Chunlei Han, Issi R Vedder, David Vállez García, Ronald Borra, et al. Software reproducibility of myocardial blood flow and flow reserve quantification in ischemic heart disease: A 13n-ammonia pet study. *Journal of Nuclear Cardiology*, 27(4):1225–1233, 2020.

[119] Tom Gyllenhammar, Marcus Carlsson, Jonas Jögi, Håkan Arheden, and Henrik Engblom. Myocardial perfusion by cmr coronary sinus flow shows sex differences and lowered perfusion at stress in patients with suspected microvascular angina. *Clinical Physiology and Functional Imaging*, 42(3):208–219, 2022.

Printed by Media-Tryck, Lund 2025 NORDIC SWAN ECOLABEL 3041 0903

About the author

Anna Székely enrolled as a research student in the Cardiac-MR group at the department of Clinical Physiology and Nuclear Medicine, Lund, Sweden, in summer 2018, while studying medicine. She continued working with research projects in the Cardiac-MR group during medical school and was enrolled as a PhD student in 2021. Since finishing medical school in the beginning of 2022, she has enjoyed a position of combined research and clinical work, which she wishes to continue during her career.

LUND UNIVERSITY

FACULTY OF MEDICINE

Department of Clinical Sciences Lund
Clinical Physiology
Lund University, Faculty of Medicine
Doctoral Dissertation Series 2025:114
ISBN 978-91-8021-767-5
ISSN 1652-8220